Uniwersytet Warszawski
Wydział Fizyki

Antoni Aduszkiewicz
Numer albumu: 215904

Operation and performance of Time Projection Chambers of SHINE/NA61 experiment at CERN

Praca magisterska
na kierunku Fizyka

Praca wykonana pod kierunkiem
dr hab. Wojciecha Dominika, prof. UW
w Zakładzie Cząstek i Oddziaływań Fundamentalnych
Uniwersytetu Warszawskiego

Warszawa, czerwiec 2008

Oświadczenie kierującego pracą
Oświadczam, że niniejsza praca została przygotowana pod moim kierunkiem i stwierdzam, że spełnia ona warunki do przedstawienia jej w postępowaniu o nadanie tytułu zawodowego.

Podpis kierującego pracą

Oświadczenie autora pracy
Świadom odpowiedzialności prawnej oświadczam, że niniejsza praca dyplomowa została napisana przeze mnie samodzielnie i nie zawiera treści uzyskanych w sposób niezgodny z obowiązującymi przepisami.
Oświadczam również, że przedstawiona praca nie była wcześniej przedmiotem procedur związanych z uzyskaniem tytułu zawodowego w wyższej uczelni.
Oświadczam ponadto, że niniejsza wersja pracy jest identyczna z załączoną wersją elektroniczną.

Data Podpis autora pracy

Abstract

This paper characterizes the Time Projection Chambers (TPC) in the SHINE/NA61 experiment at CERN and their operation during the first run in 2007. An analysis of a change of the gas mixture in the TPCs for SHINE is included. Also the gas system of the TPCs is described.

Streszczenie

W pracy opisane są komory projekcji czasowej (TPC) eksperymentu SHINE/NA61 w CERNie i ich działanie podczas pierwszego runu w 2007 roku. Przedstawiona jest analiza mieszanki gazowej w komorach TPC wybranej w SHINE. Szczegółowo omówiony jest też system gazowy tych komór.

Polski tytuł pracy:

Działanie komór projekcji czasowej (TPC)
w eksperymencie SHINE/NA61 w CERNie.

Słowa kluczowe

NA61, SHINE, NA49, NA49-future, komora projekcji czasowej, TPC, system gazowy

Dziedzina pracy

13200 Fizyka

Contents

1 Introduction

1.1 Background

SHINE (**S**PS **H**eavy **I**on and **N**eutrino **E**xperiment) [1] is the official name of the NA61 experiment located in the **N**orth **A**rea of the CERN SPS accelerator. SHINE is a continuation of the NA49 experiment. The main part of the detector consists of time projection chambers (TPC) – gas detectors able to detect tracks of over 1000 particles from a single nuclear collision.

The first section of this paper introduces the experiment, its history and gives an overview of the detector. Section 2 describes the basics of TPC operation and signal reconstruction. It explains why a stable and pure gas mixture is necessary to achieve good resolutions. Also an analysis of the detector performance with the gas mixtures chosen for SHINE is presented in section 2.5. Section 3 contains a detailed description of the gas system of the TPCs and its parts. Results of the operation of the system during the SHINE run in 2007 are included.

Due to the new experimental program, the institutional collaboration of SHINE differs with respect to NA49. Expertise should be gained on the technical aspect of the apparatus. In particular nobody in the new collaboration has serious experience in operating the complex gas system. The documentation of the system consisted only of routinely filled logbooks. It was a huge task to understand the operation of the system and the function of its elements. Author of this paper was responsible for starting the gas system of the TPCs in 2006 after a few years of inactivity and for maintaining and operating the system during the runs in 2006 and 2007.

1.2 NA49 experiment

NA49 was a fixed target experiment located in north area of the CERN SPS accelerator. It has been designed for the study of hadron production in p+p, p+A and A+A collisions at energies 20-200 GeV/A[1] (maximum of 158 GeV/A for the heaviest used nucleus: Pb) [2].

[1] Energy per nucleon of the projectile.

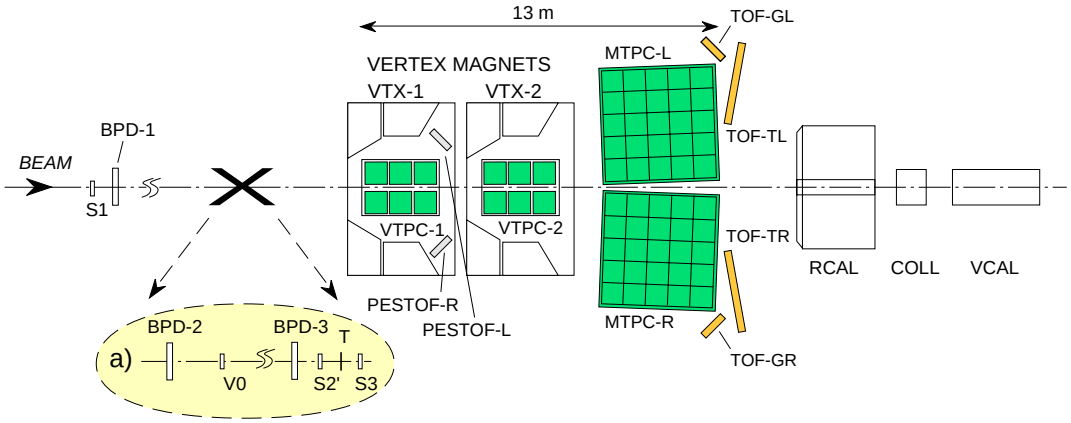

Figure 1: A bird's eye view of of NA49 detector. Beam particles arrive from the left side, pass through trigger counters and beam position detectors, then hits the target. Products of the collision are detected in 4 TPCs (green), TOF walls (yellow) and 2 calorimeters. The "GAP" TPC is not shown – it has been added in a later stage of the experiment.

NA49 was taking data from 1995 to 2002.

1.2.1 Beam detection and triggering

A schematic view of the NA49 detector is presented in fig. 1. Beam particles are identified by two Čerenkov detectors (not shown in the figure) and three Beam Position Detectors (BPD). The BPDs are 3×3 cm^2 proportional chambers with cathode strip readout. Two orthogonal sense wire planes are sandwiched between three cathode planes. The total charge readout from a BPD allows beam particle identification by analysis of energy loss. The individual beam particle position measured in the three detectors allows the reconstruction of the interaction point in the target with a precision of 40 μm for proton beams (170 μm for Pb beams).

Signals from the Čerenkov detectors and a set of scintillator counters allow to form a trigger. Beam particles are detected using the Čerenkov detectors and scintillator counters placed on the beam line. An additional scintillator counter with a hole centered on the beam line allows to reject poorly collimated beam particles. The last scintillator counter is located on the beam line, behind the target. If a beam particle is detected, the lack of a signal from the last counter identifies an interaction and triggers the event readout.

Table 1: Dimensions of VTPCs and MTPCs

Dimensions [mm]	VTPC-1	VTPC-2	MTPC-L/R
Width	2 000	2 000	3 900
Length (parallel to the beam line)	2 500	2 500	3 900
Height	980	980	1 800
Drift length [mm]	666	666	1 117

1.2.2 Time Projection Chambers

The main detectors measuring charged products of an interaction are five Time Projection Chambers (TPC): "vertex" TPCs: VTPC-1, VTPC-2, "main" TPCs: MTPC-L(eft), MTPC-R(ight) and GAP TPC. They are gas detectors allowing for precise (few hundred μm spatial accuracy of point position) three-dimensional measurement of tracks of charged particles emitted from the interaction. Over 1000 tracks can be reconstructed in one Pb+Pb interaction. A detailed description of the TPC operation is presented in section 2.

The dimensions of the TPCs are presented in table 1. Each VTPC has two active sections with a 25.5 cm wide inactive gap between; the beam passes through this inactive gap. The GAP TPC is centered on the beam line measuring particles down to the smallest production angles.

Both VTPCs and the GAP TPC are located inside two superconducting dipole magnets. The magnetic field is parallel to the electric field. This allows ionization electrons to drift parallel to the electric field; the magnetic field does not affect the drift direction. Only in the corners of the VTPCs the magnetic field is inhomogeneous and corrections have to be applied. The magnetic fields for 158 GeV beam energy equals 1.5 T in the upstream magnet and 1.1 T in the downstream magnet. The field is reduced for lower beam energy. The magnetic field bends the tracks of charged particles allowing to measure their momenta. Typical resolution vary from $dp/p^2 = 7.0 \cdot 10^{-4}$ (GeV/c)$^{-1}$ for tracks detected in VTPC-1 only, down to $dp/p^2 = 0.3 \cdot 10^{-4}$ (GeV/c)$^{-1}$ for tracks detected in VTPC-2 and one of the MTPCs.

TPCs also allow for the measurement of the energy loss in gas (dE/dx). This is the main function of the MTPCs: they are outside of the magnetic field, so the tracks are straight. However, thanks to their large size they allow to register up to 90 samples of energy loss

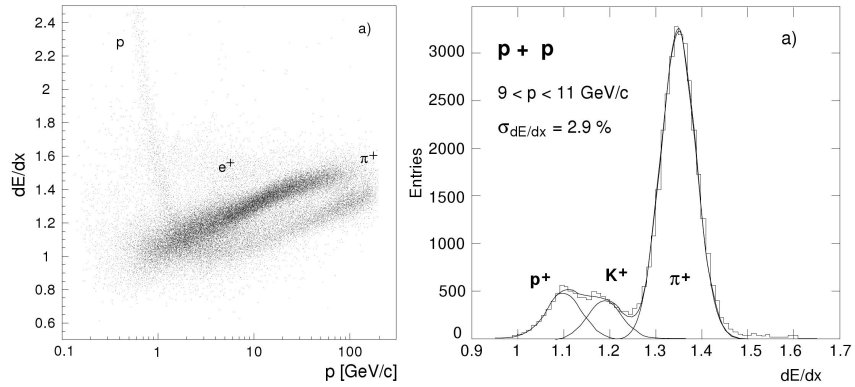

Figure 2: Particle identification: The plot on the left side shows the energy loss (dE/dx) of positive particles in TPCs as a function of momentum for p+p interactions. Bethe-Bloch curves for various types of particles are clearly visible. The plot on the right side shows dE/dx distribution in the momentum range 9-11 GeV/c. The plots show data measured in the NA49 TPCs. dE/dx is shown in arbitrary units. [4]

per track, providing high statistics for precise measurement. The energy loss of moderately relativistic particle ($0.5 < \beta\gamma < 500$) is described by the Bethe-Bloch formula: [3]

$$-\frac{dE}{dx} = Kz^2\frac{Z}{A}\frac{1}{\beta^2}\cdot\left[\ln\frac{2m_e c^2\beta^2\gamma^2 T_{\max}}{I^2} - \beta^2 - \frac{\delta(\beta\gamma)}{2}\right] \tag{1}$$

where $\gamma = (1-\beta^2)^{-1}$, $\beta = v/c$, v – velocity of the particle, c – speed of light, x – distance travelled by the particle, ze – particle charge, e – charge of the electron, Z – atomic number of absorber, A – atomic mass of absorber, m_e – mass of the electron, $T_{\max}$ – maximum kinetic energy that can be imparted to a free electron in a single collision, I – mean excitation energy of absorber, K – constant, $\delta(\beta\gamma)$ – density effect correction to ionization energy loss.

The formula (1) depends on velocity of a particle. The combination of momentum measured from the track curvature and the dE/dx measurement allow for particle identification. An example is presented in fig. 2.

1.2.3 Time-Of-Flight

Behind the TPCs there are Time-Of-Flight (TOF) detectors. They are scintillator detectors allowing to measure the arrival time of particles with a precision of 60 ps. The independent measurement of particle velocity is obtained by dividing the distance from the interaction point by the time between the beam detection and the arrival of the particle. Velocity and

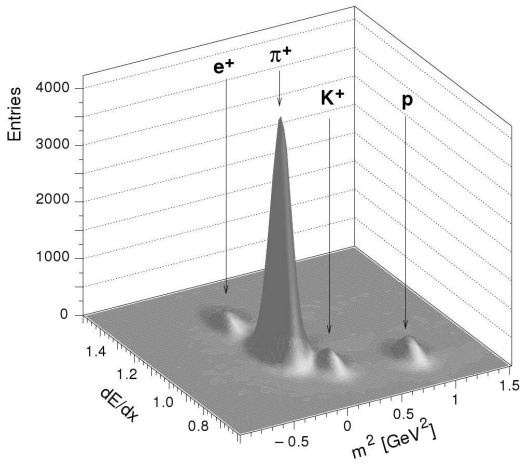

Figure 3: dE/dx and TOF (square mass) measurement in the momentum range 5-6 GeV/c for central Pb+Pb collisions. Combining the two methods improves efficiency of the particle identification. [4]

momentum allow to calculate the mass:

$$p = \frac{\beta}{\sqrt{1-\beta^2}} \cdot mc \Rightarrow m^2 = \left(\frac{p}{c}\right)^2 \left(\frac{1}{\beta^2} - 1\right) = \left(\frac{p}{c}\right)^2 \left(\frac{c^2 t^2}{s^2} - 1\right), \tag{2}$$

where p – momentum, m – mass, $\beta = v/c = s/(ct)$, t – time of flight, s – length of flight, c – speed of light. Therefore TOF used together with TPCs improves precision of particle identification, especially or minimum ionization particles $\beta\gamma \approx 3$. Fig. 3 shows particles identified using this method.

In NA49 there were also PesTOF counters located between the VTPCs. They were spark counters. Their resolution reached below 50 ps. They improved particle identification in the backward hemisphere (in center of mass), particularly separation between protons and kaons.

1.2.4 Calorimeters

There were 2 calorimeters in NA49 [5]:

- **Ring calorimeter** (RCAL in fig. 1) consisting of electromagnetic and hadronic calorimeters. It was used for the measurement of neutral particles in p+p and p+A collisions, and for transverse energy determination and event anisotropy measurement in high multiplicity Pb+Pb collisions.

- **Veto calorimeter** (VCAL) used for the selection of central Pb+Pb interactions. The

calorimeter measured the energy of the fragments of projectile nuclei that have not interacted with the target ("spectators"). The geometrical acceptance of the VCAL calorimeter was adjusted for each energy in order to cover the projectile spectator region by a proper setting of a collimator (COLL).

1.3 SHINE experiment

1.3.1 Motivation to continue the experiment

Data-taking of NA49 was finished in 2003, but it turned out that the existing detector can be used for the new experimental program. The main issues of the physics motivation are [6] [7]:

- **Search for critical point of the quark-gluon plasma phase transition and study of the onset of deconfinement in nucleus-nucleus collisions:** NA49 measurements of hadron production in central Pb+Pb collisions at energies 20-158 GeV/A showed evidence for the existence of a Quark Gluon Plasma (QGP) – a new state of strongly interacting matter. There is also the possibility of the existence of a critical point of transition between QGP and hadron matter. This point could exist in the temperature and baryonic chemical potential space, and it could be found by an experimental scan in the energy and system size space. The energy of the projectile can be varied from 10 to 158 GeV at the SPS. The size of the system can be changed by varying the species of interacting nuclei. Interactions of p+p, C+C, Si+Si and In+In are planned. A visualisation of the data-taking plans is shown in fig. 4.

- **Measurement of hadron production in p+p and p+Pb interaction at 158 GeV:** such measurement is necessary for better understanding of nucleus-nucleus reactions. The high statistic ($5 \cdot 10^7$ events) data will be used for study of correlations, fluctuations and production of particles produced with high transverse momenta.

- **Collecting reference data for the T2K experiment:** T2K is an experiment planned to be launched in 2009. It will measure the properties of neutrino oscillations, in particular the θ_{13} angle of neutrino mixing. The experiment is located in Japan. A

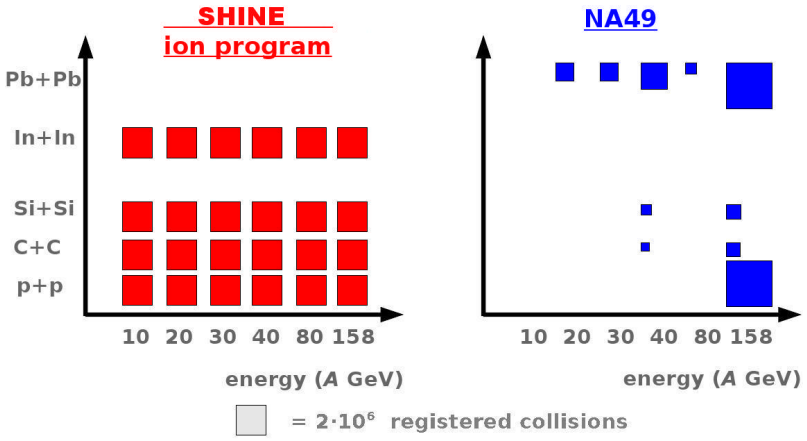

Figure 4: The SHINE data taking program for QGP physics. A two dimensional scan (colliding system size versus energy) may reveal the critical point of QGP transition. The data already taken by NA49 are presented on the right side for comparison.

neutrino beam will be produced at J-PARC accelerator in Tokai from the decays of pions created in the interactions of 30-50 GeV protons with a carbon target. Neutrinos will be detected in the Super-Kamiokande detector 295 km away.

In order to reduce the uncertainty of this measurement it is crucial to know precisely the composition of particles coming out from the p+C interactions. Especially important is the understanding of the kaon content: muon neutrinos from kaon decay will be background for the measurement of muon neutrinos from $\pi^{\pm}$ decays. The NA49 detector can be used to study p+C interactions at the same energies as in the T2K experiment. Precise measurement of cross-sections and branching ratios can significantly decrease the T2K systematical uncertainties.

- **Collecting reference data for the Pierre Auger experiment:** Pierre Auger is a cosmic ray experiment located in Argentina. It detects cosmic rays by measuring particle "showers" reaching the ground and ultraviolet light emitted high in the atmosphere. The incoming cosmic ray particle is measured indirectly; the information of particles reaching the ground is used to reconstruct the shower. A systematical uncertainty comes from the models used for simulations. The GHEISHA model (used for low energy interactions) and QGSJET (used for high energy interactions) give different results at energies around 80 GeV. The SHINE detector allows for a precise particle identification. The measurement of p+C interactions at 400 GeV will con-

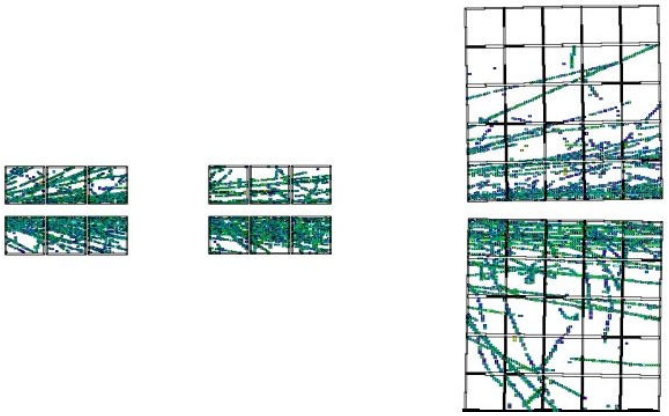

Figure 5: Example of an event measured during NA49-future test run in 2006. The magnetic field was turned off during the test run, so the tracks in the VTPCs are straight. The lack of points in 5 sectors of MTPC-L is caused by temporary problems with power supplies of the readout electronics.

siderably reduce the uncertainties of models used by Pierre Auger and other cosmic ray experiments.

1.3.2 NA49-future

In August 2006 a technical test run of so called NA49-future experiment took place. The purpose of the test was to check whether the detector was still operational and could be used for a physics program. The trigger system, vertex and main TPCs and the first module of a new calorimeter were tested.

For simplicity during the test run a mixture of Ar/CO_2 95/5 has been used in the MTPCs instead of $Ar/CH_4/CO_2$ 90/5/5 which had been used in NA49. It turned out that the new mixture provided comparable signal quality and that it could be used in further runs. A detailed analysis of the new gas mixture is presented in section 2.5.

The test included the trigger system, BPDs and TPCs. Also the first module of the Projectile Spectator Detector (PSD) calorimeter was tested. The magnets and TOF walls were not tested. An example of an event measured during the run is presented in fig. 5.

The test run was successful. The new experiment NA61/SHINE was approved.

1.3.3 SHINE

The first run of SHINE took place in October 2007. The main scope was to take statistics for neutrino production calibration in the T2K experiment: p+C interactions at 30.9 GeV.

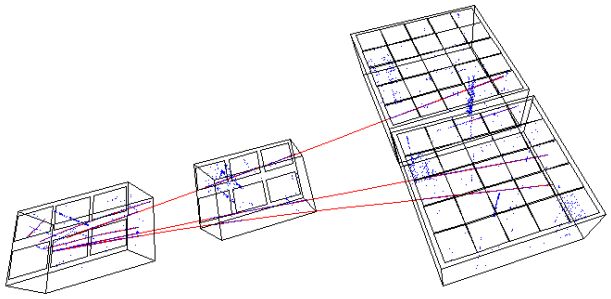

Figure 6: Example of an event measured during the first SHINE run in 2007. Red lines show reconstructed tracks.

The data were taken using a 2 cm length carbon target ($6.6 \cdot 10^5$ events) and a 90 cm length replica of the carbon target which will be used in T2K ($2.3 \cdot 10^5$ events).

During the run the detector basically functioned properly. An example of an event measured during the run is shown in fig. 6. The data acquisition was slower than predicted, but the collected amount of data is sufficient for a pilot analysis. The problem of the limited speed of data acquisition will be eliminated in the next years due to the upgrade of the data acquisition system. During the calibration analysis of the data an inconsistency of the drift velocity measured in the monitor counters and the one reconstructed from the MTPC data appeared. This problem is still under investigation; it is described in detail in section 3.3.2. A super-module (3×3 array) of the PSD calorimeter was successfully tested.

During the run in 2008 further data taking for T2K is planned. Also p+C interactions at 400 GeV will be measured. The high statistics measurement of p+p and p+Pb collisions will begin and it will be continued to 2009. The nuclei+nuclei interactions for QGP physics will start in 2010 and will be continued in further runs.

1.4 SHINE detector overview

The scheme of the SHINE detector is presented in fig. 7. The main parts (TPCs, TOF, BPD and magnets) are the original NA49 apparatuses [4], some parts are (or will be) upgraded:

- New **"forward" time of flight** increasing the detector acceptance in the region (small angles) important for neutrino physics.

- New **Projectile Spectator Detector (PSD) calorimeter**. The new calorimeter is

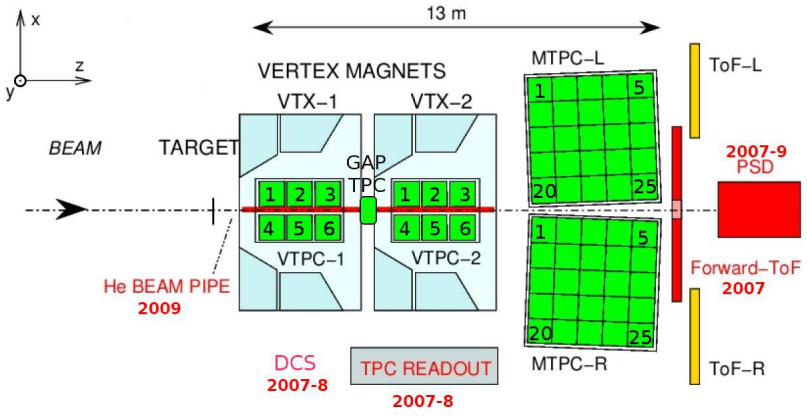

Figure 7: A bird's eye view of of the SHINE detector. A major part of the detector comes from NA49 experiment: 5 TPCs (green), outer TOF walls (yellow) and the magnets. New parts and the planned upgrades are drawn with red color: the "PSD" calorimeter, central TOF wall and helium pipe. The sector numbering convention in the TPCs is presented (6 sectors in each VTPC and 25 in each MTPC).

necessary for QGP physics. One of the signatures of the critical point of QGP transition are fluctuations of the charged particles multiplicity. Simulations showed that PSD will decrease the uncertainty of the measured fluctuations by a factor 5 or more.

PSD is a sampling calorimeter. It is made of $10 \times 10 \times 120$ cm^3 scintillator (4 mm layers) sandwiched with Pb (16 mm layers) modules. The light from the scintillators is transmitted via WLS-fibers to the readout micropixel avalanche photodiodes (MAPD).

One prototype module was tested during test run in 2006, 9 modules were tested during the run in 2007, the final detector consisting of 108 modules should be constructed in 2009. It is expected that the final calorimeter will have a resolution $\sigma(E)/E < 50\%/\sqrt{E\ [GeV]}$, and very good transversal uniformity. The NA49 Veto and Ring calorimeters are no longer used in SHINE.

- New, **faster data acquisition system**. In order to achieve physics goals, large amounts of data have to be taken. With the new data acquisition it is expected that the recorded event rate will increase from a few Hz to over 100 Hz.

- **Helium pipe** for the beam passing through the VTPCs, reducing the number of δ electrons in the TPCs and reducing the probability for interaction between the target and the calorimeter. The δ electrons will be a bigger problem in SHINE than they

were in NA49. The beam intensity will be increased about 100 times. This will increase production of δ electrons proportionally. The electrons will ionize gas in the TPCs. This will increase the event size, impede the track reconstruction and cause track distortions due to space-charge effects. The helium pipe is planned to be installed in 2009.

- **Reduced TPC sampling rate** from 512 timebins to 256 timebins to limit the amount of the data in each event. A smaller amount of data in a single event buffer will allow for faster data acquisition. The reduction is possible, because in NA49 the mean number of time slices in a cluster equaled 6. After the upgrade the mean number of time slices is reduced to 3, which is sufficient for precise cluster localization[2].

2 Time Projection Chamber detector

2.1 Introduction

The Time Projection Chamber (TPC) is a gas detector for charged particles. It allows to reconstruct tracks in three dimensions. A large TPC can measure many particles at the same time: in NA49 in average over 1000 tracks were recorded in a single Pb+Pb collision. [8]

2.2 Construction and principle of operation

2.2.1 Primary ionization

The principle of particle detection is illustrated in fig. 8. The volume of the TPC is filled with gas. A high-energy charged particle passing through the drift volume ionizes the atoms and the molecules of the gas. There is a uniform electric field in the drift volume of the TPC. The electrons from the ionization drift towards the readout pads.

[2]Definitions of *time slices* and *clusters* are presented in section 2.3

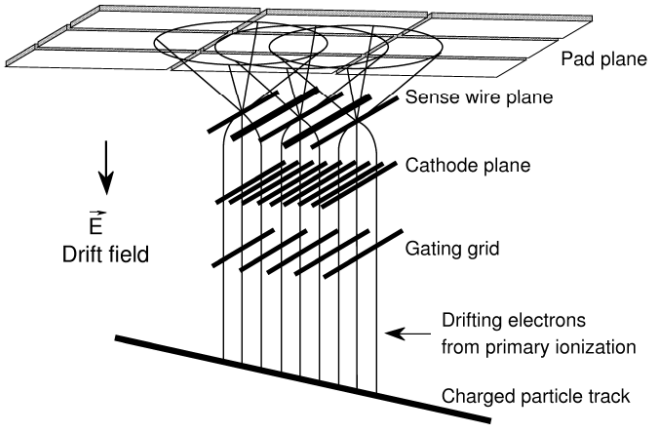

Figure 8: Particle detection in a TPC: a charged particle ionizes the gas in the drift volume. The electrons drift towards the multiwire proportional chamber on the top of the TPC. They are amplified on the sense wires and signal is induced on the readout pads.

2.2.2 Field cage

The drift volume is surround with electrodes shaping the electric field inside. The grounded "cathode plane" visible in fig. 8 closes the field from the readout pads' side (it is in fact an anode from the point of view of the field cage). The side walls of the drift volume are closed with aluminized Mylar strips of 25 μm thickness and 0.5 inch width. They are arranged perpendicularly to the drift direction. Voltage applied to them is gradually decreasing with the distance from the cathode plane down to about -19 kV in MTPCs and -13 kV in VTPCs. The voltage on the strips is applied using a resistor voltage divider chain. The plane of aluminized Mylar strips of the same type closes the field cage. The full drift voltage is applied to this plane, thus defining the electric field in the TPC.

The TPCs in SHINE are orientated so that the readout pads are on the top of the chambers. The drift field is pointed downwards so the electrons from the ionization drift upward. The drift lengths are listed in table. 1.

2.2.3 Charge collection

There is a multiwire proportional chamber (MWPC) in the upper part of the drift volume: near the readout pads there are sense wires connected to high voltage. The wires are very thin (20 μm in case of SHINE) so the density of electric field lines close to them is very high. Electrons approaching the wires gain energy allowing them to ionize further

molecules. This process repeats itself creating an avalanche of 10^3-10^6 electrons from each electron from the primary ionization. The process is called *gas amplification* (or *gas gain*). When the electrons from the avalanche hit the wire they induce an electromagnetic pulse on 3-4 closest readout pads.

2.2.4 Gating grid

The gating grid wires allow to select the events. The gate is open only during the collection of charge from the drift volume. To open the gate, equal voltages are applied to all the gate wires, providing very effective charge transmission from the drift volume to the MWPC volume. To close the gating grid the wires are polarized alternatingly with positive and negative voltage (order of ±50 V). Electrons from the drift volume are attracted to the wires rather than pass through the grid.

The gating grid is open only for 50 μs in each event. This imposes constraints on minimum drift velocity in order to collect the charges from the whole depth of the TPC. Closing the gate between events prevents unnecessary gas amplification which could cause ageing effects on the wires. Also it reduces amount of positive ions getting into the drift volume from the charge avalanches. The positive ions drift about 3-4 orders of magnitude slower than electrons. They stay in the drift volume for relatively long time causing *space charge effects* which distort the drift field. This effect has not been observed in NA49 due to low interaction rate.

2.2.5 Sectors and pads

The SHINE standard coordinate system is: z is horizontal, parallel to the beam line, y is pointing up – parallel to the drift direction, and x is the second horizontal coordinate, perpendicular to the beam line and the drift direction. The coordinates are shown in fig. 7. The (0, 0, 0) point of the system is on the beam line, at the center of VTPC-2.

The TPCs are subdivided into sectors. Each sector has an individual multiwire chamber. The sector numbering convention is presented in fig. 7.

Table 2: Properties of pads in VTPCs and MTPCs

Dimensions [mm]	VTPC-1	VTPC-2	MTPC-L/R
Pad length	16, 28	28	40
Pad width	3.5	3.5	3.6, 5.5
Pad angles	5-55°	3-20°	0°, 15°
Number of pads	26 886	27 648	63 360

The readout pads are rectangles or trapezia[3] elongated parallel to the beam line (dimensions and tilt angles are listed in table 2). The uncertainty of cluster position increases with the angle between the track and the pad so the tilt angle of the trapezoidal pads is optimized to minimize this angle for most of the tracks:

- **VTPC-1** All pads are 3.5 mm wide (in the direction perpendicular to the beam). Pads in the sectors 1 and 4 (closest to the target) are 16 mm long; pads in other sectors are 28 mm long. The tilt angle is adjusted individually for each pad as a function of x and z coordinates; it varies from 5° to 55° in various regions of VTPC-1.

- **VTPC-2** All pads are 3.5 mm wide and 28 mm long. The tilt angle increases linearly with the distance from beam line ($|x|$): from 3° to 20°.

- **MTPC-L/R** All pads are 40 mm long. The five sectors closest to the beam line (21-25 in MTPC-L and 1-5 in MTPC-R) are called *high resolution*. The pads are 3.6 mm wide and are not tilted.

  The further five sectors (16-20 in MTPC-L and 6-10 in MTPC-R) are called *standard resolution*. The pads are 5.5 mm wide and are not tilted.

  The remaining sectors (1-15 in MTPC-L and 11-25 in MTPC-R) are called *standard resolution prime*. The pads are 5.5 mm wide and are tilted by a constant angle of 15°.

2.3 Data readout and reconstruction

There are in total 181 254 pads in the four TPCs (not counting the GAP TPC). A single readout of all pads is called *time slice*. In each event 256 (512 in NA49) time slices are

[3] *trapezium* word is used in British English meaning: "a quadrilateral with one pair of sides parallel" according to "The New Oxford Dictionary of English", Oxford University Press 1998, p. 1971.

Table 3: Selected properties of gases used in NA49 and SHINE: t_{99}: thickness of the gas layer for 99% efficiency of ionization and average number of free electrons produced by minimum ionization particle. [3]

Gas	t_{99} [mm]	free electrons/cm
Ne	3.8	42
Ar	1.8	103
CH_4	1.7	62
CO_2	1.3	107

taken during the readout time of 50 μs. The pads are being read using 8-bit ADC. This results in over 44 MB of data from each event.

Electrons from the primary ionization drift towards the readout pads with constant velocity. Therefore the time between the beginning of an event and signal detection allow to calculate the drift length – y coordinate of particle passing through the TPC. A single time slice corresponds to about 2.6 mm in VTPCs and 4.4 mm in MTPCs. The position of the pad gives information about x and z coordinates.

The signal is analysed independently in rows perpendicular to the beam line (so called *padrows*). Signal from the gas amplification is induced on a few adjacent pads. Also the preamp-shaper circuit connected to the pad increases the duration of the registered pulse. The resulting detected signal has a width of a few pads and a few time slices. Such two dimensional (x – depending on pad position in a padrow, y – depending on time slice) group of signals generated by one particle and measured in one padrow is called a *cluster*. Calculating mean x and y position of a cluster allows for obtaining resolution much better than the size of pad and time slice: the uncertainty of cluster position varies between 0.1-1.4 mm. The uncertainty depends on the region of the TPC, drift length, number of pads in the cluster and angles between track and pad plane and pad tilt angle.

2.4 Operational aspects of the gas mixture

The particle detection in TPC is based on a few phenomena: ionization, electron drift and gas amplification. Achieving a good quality of the signal is possible if the gas mixture fulfills the following conditions:

- Ionization and gas amplification must be sufficiently high in order to allow to register

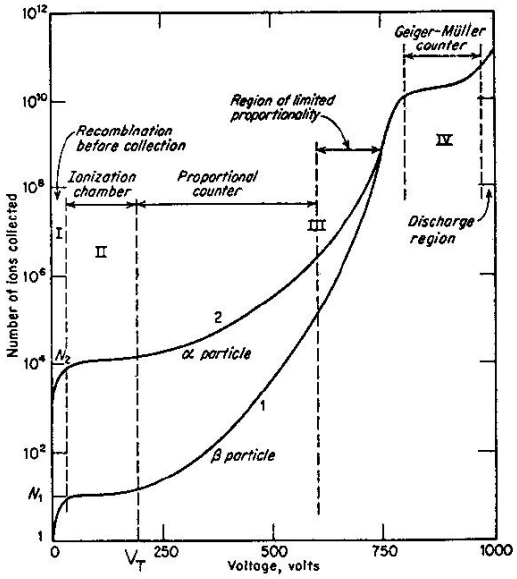

Figure 9: Typical number of electrons collected on the sense wire. The detector behaviour depends on the voltage: *I* If the voltage is too low, drifting electrons recombine to molecules and signal is lost; *II* If the voltage is higher most electrons reach the wire, but there is still no amplification; *III* Above a certain voltage (V_T) gas amplification is possible, the number of collected electrons is proportional to the number of the primary electrons. However a further increase of voltage causes loss of this proportionality; *IV* For higher voltages each primary ionization cause sparks between anode and cathode. All information about the number of primary electrons is lost, the detector can work only as a Geiger-Müller counter. For even higher voltages discharges may appear spontaneously. A discharge can damage the detector designed to work in the proportional mode. [9]

the signal. These processes depend strongly on the gas mixture used. The properties of the gases used in the experiment are presented in table 3.

- In order to obtain a signal suitable for dE/dx analysis, the gas amplification must work in the proportional mode. Also the signal has to be contained within the dynamic range of the ADC. A plot of the typical number of electrons collected on a sense wire as a function of the applied voltage is shown in fig. 9. However variations of the distances between the pad plane, the sense wire plane and the cathode plane cause variations in the signal amplitude up to 20%. The high voltage is set independently for each sector of the TPCs, but the detector sensitivity varies from pad to pad. The shape of the plot shown in fig. 9 depends on the gas mixture. Therefore a stable gas mixture is required to allow to set the high voltage values properly.

- The drift velocity must be kept high enough in order to allow to read the whole depth of the chamber during the 50 μs of charge collection: 1.4 cm/μs in the VTPCs and 2.4 cm/μs in the MTPCs. Moreover, the drift velocity must be very stable over time

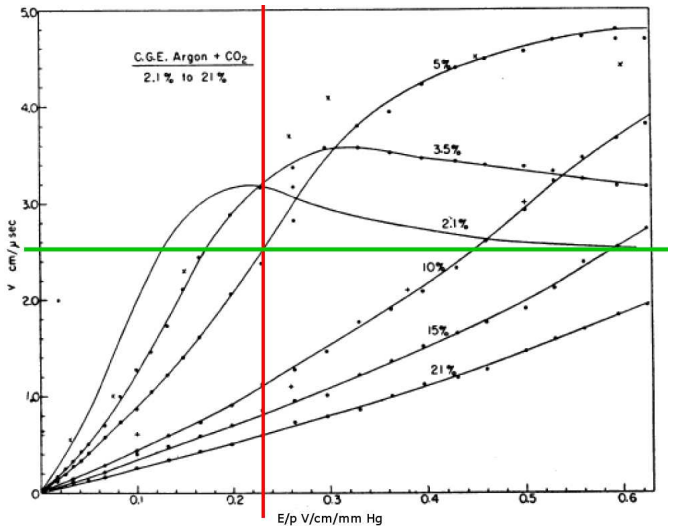

Figure 10: Dependence of the drift velocity on the "reduced drift field" (electric field divided by gas pressure) for various Ar/CO_2 mixtures. The horizontal green line shows the optimal drift velocity for the MTPCs. [10]

to allow for accurate calculation of vertical cluster coordinate. The dependence of drift velocity on the reduced drift field and gas mixture is presented in fig. 10. In most cases the drift velocity can be increased by increasing the drift voltage, but there are limits: the high voltage cables used in the experiment can be used safely to up to 30 kV (which corresponds to about 0.36 V/cm/mm Hg at atmospheric pressure). Excessive voltage may cause excessive heating of the resistor divider chain the voltage in the TPCs; however this effect has not been noticed up to 20 kV. Another limitation is the design of the field cage: at some point discharges to ground may occur from the high voltage side. No tests have been done, but caution is mandatory when applying high values the drift voltage.

High drift velocity can be obtained using argon, neon and methane (CH_4). The drift velocity decreases significantly with increasing CO_2 admixture.

- Diffusion of the electrons during the drift should be kept on low level in order to prevent unwanted cluster size increase, which – in turn – deteriorates the spatial resolution and the two-track-resolution. During the gas amplification process also photons are produced. They can initiate further electron avalanches increasing the risk of a discharge. Both these problems can be reduced using a so called *quenching gas*, for example CO_2 and/or CH_4.

Table 4: Gas mixtures used in the experiment

TPC	NA49	NA49-future test run in 2006	SHINE run in 2007
VTPC-1/2 GAP TPC	Ne/CO_2 90/10	Ar/CO_2 90/10	Ar/CO_2 90/10
MTPC-L/R	$Ar/CH_4/CO_2$ 90/5/5	Ar/CO_2 95/5	Ar/CO_2 94/6

Methane does not cause a decrease of drift velocity as CO_2 does. However using methane may cause ageing effects on the readout wires (fortunately this effect has not been observed in NA49 yet). Also it is a flammable gas and using it requires certain safety measures.

- The oxygen impurity in the working gas should be kept low. Oxygen is electronegative and each ppm of oxygen causes up to 1.2% loss of drifting charge for the full drift length in the MTPCs. Charge loss due to water contamination is much lower – about 2% per 100 ppm. [4]

2.5 Gas mixture in SHINE TPCs

2.5.1 Motivation for choice of the gas mixture

Gas mixtures used in the experiment are listed in table 4. During the NA49-future test run in 2006 methane was not used in order to avoid security problems. Also – for simplicity – argon was used in VTPCs instead of neon. The purpose of the test run was only to verify the status of the detectors after a few years of shutdown. However, the obtained signal quality was comparable to the results from NA49. It turned out that for the low multiplicity of particles TPCs can work using the simpler gas mixture.

In VTPCs neon is just replaced by the same fraction argon, that has comparable properties. The reason for using neon in NA49 was to reduce multiple scattering and reduce number of δ electrons in Pb+Pb interactions with high track multiplicity. This will be less of a problem in low multiplicity light ions interactions in SHINE. The problem of δ electrons will be also reduced by helium pipe.

The change of the gas mixture in the MTPCs was more controversial: the argon content

was increased from 90% to 95% and the amount of quenching gas was decreased by half. A reduction of quenching gas admixture decreases the range of voltages on the sense wires where they can operate in the proportional mode. This – in turn – increases the risk of sparks that could be dangerous for the chamber operation. After the NA49-future test run an analysis of signal quality was done.

2.5.2 Test run results

To study the TPC detection properties for selected gas mixture, tests were performed for several voltages applied to the sense wires in the MTPCs:

- ▲ 1100V/1030V (standard resolution sectors/high resolution sectors) – marked with red triangles on the plots (runs 5018-5021),
- ● 1080V/1010V – marked with blue circles (runs 5056-5059),
- ■ 1060V/990V – marked with green squares (runs 5101-5107, 5109).

The data from the test run was compared to the NA49 data from p+Pb interactions at beam energy 158 GeV (run 4398) (marked with black stars (⁎) on the plots).

The following parameters of the clusters were investigated:

- *Number of pads in a cluster* – cluster width in x (horizontal) dimension, integrated over time slices (y),
- *Number of time slices of a cluster* – cluster width in y (vertical) dimension, integrated over pads (x),
- *Maximum ADC reading in cluster.* An important parameter is *overflow* – fraction of clusters exceeding the range of the 8-bit ADC. In such clusters the information about the charge is distorted. An example of the distribution of the maximum ADC value in a cluster is presented in fig. 11.

The analysis of the cluster characteristics was done independently in each of the 25 sectors of each MTPC, in 5 horizontal "slices". This allowed to measure the cluster properties dependence on drift length. The results are presented in fig. 12 (number of pads and

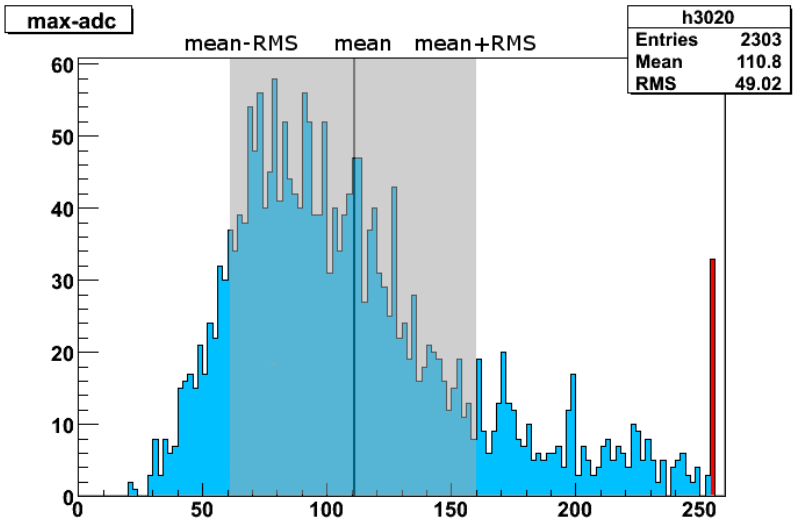

Figure 11: Example distribution of maximum ADC reading in a cluster. The mean value is marked by dark vertical line, the shaded area shows ±1 RMS around the mean value. One can see large value in the 256th bin, marked with red color – this is result of 8-bit ADC overflow. An *overflow* value used later in the analysis is calculated as ratio of overflowed clusters (red bin) to all clusters (blue bins + red bin).

time slices) and fig. 13 (maximum ADC and overflow) for MTPC-L and figs. 14 and 15 for MTPC-R. It is clearly visible that the values vary systematically from sector to sector. Therefore weighted means of the ratios of values from NA49-future test run to NA49 reference have been calculated. The ratios for the high resolution sectors deviate strongly from the rest of the sectors so their means have been calculated independently. Unfortunately, due to the technical problems with the power supplies of the electronics during the test run, data from some sectors is unavailable, in particular from the MTPC-R high resolution sectors. These problems were unrelated to the gas mixture and have been solved before the first SHINE run.

The resulting plots 16-23 show the data from the NA49-future test run normalized to the NA49 data. Values on the plots are close to 1 in most cases, which means, that the new gas mixture allows to obtain comparable signal quality. A detailed analysis is presented below.

- *Number of pads in a cluster.* The results are presented on figs. 16 and 17. The normalized numbers of pads for the lowest voltage (■) are the lowest on all of the plots, they are also close to 1. Values for the higher voltages (●, ▲) are above. Larger number of pads means larger cluster width. This can lead to lower resolution in the

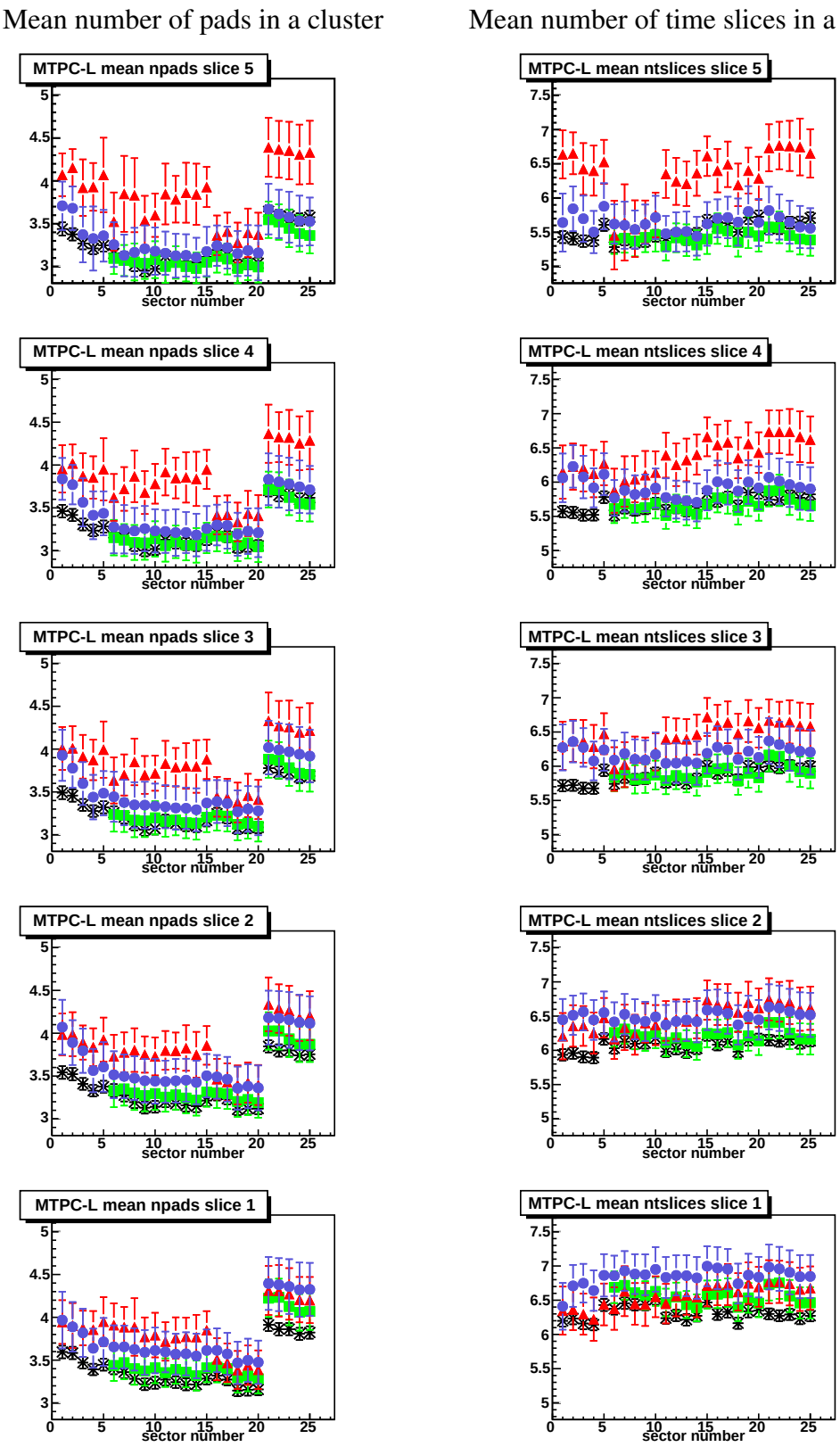

Figure 12: Mean number of pads and time slices in a cluster in MTPC-L. The plots represent 5 different horizontal slices of the MTPC: The lowest one corresponds to the longest drift length, the topmost to the shortest drift length. Black stars are NA49 reference data, and green, blue and red points are NA49-future data. The horizontal axis on each plot is the sector number.

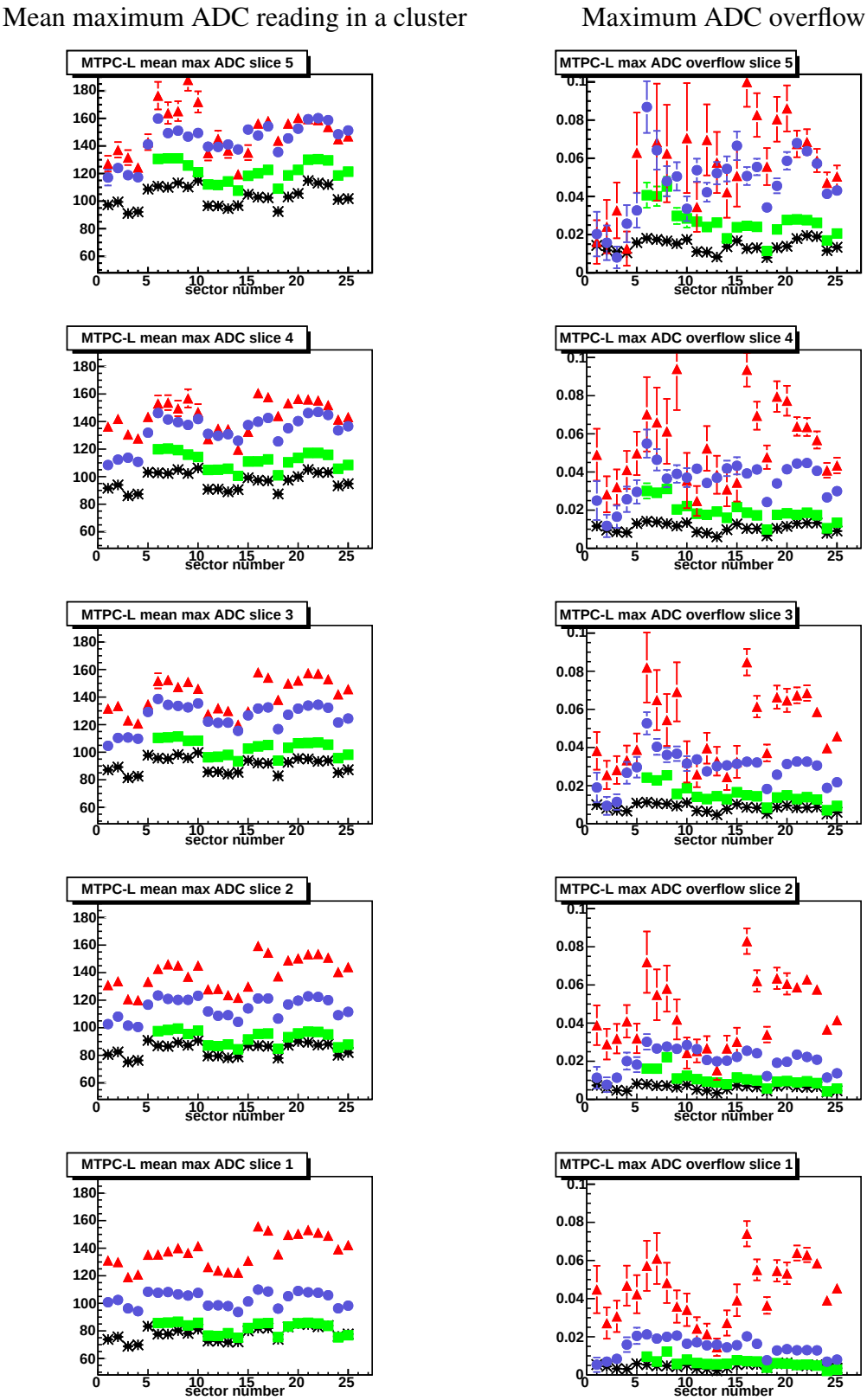

Figure 13: Maximum ADC reading in a cluster and fraction of overflowed clusters in MTPC-L. The plots represent 5 different horizontal slices of the MTPC: The lowest one corresponds to the longest drift length, the topmost to the shortest drift length. Black stars are NA49 reference data, and green, blue and red points are NA49-future data. The horizontal axis on each plot is the sector number.

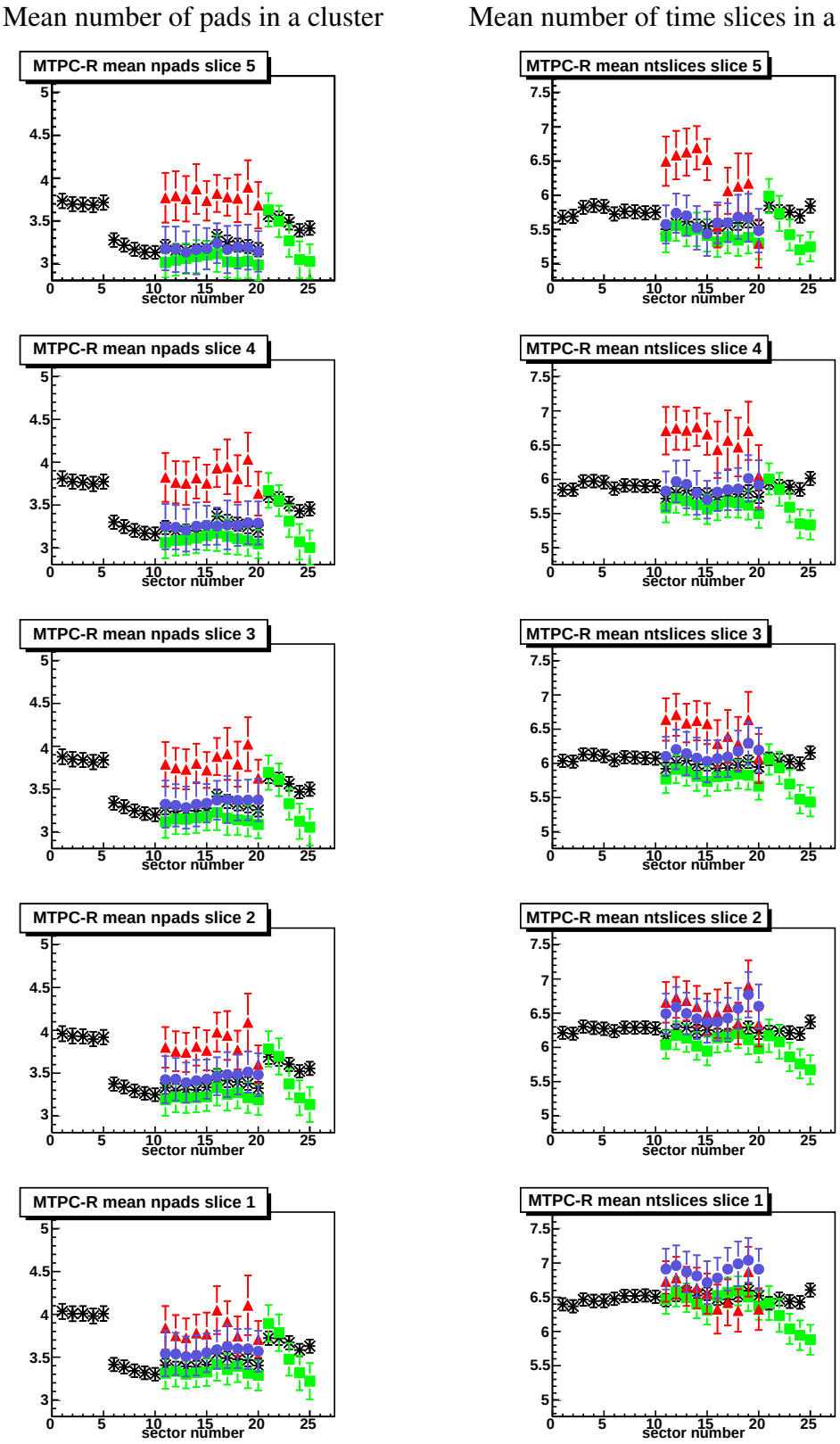

Figure 14: Mean number of pads and time slices in a cluster in MTPC-R. The plots represent 5 different horizontal slices of the MTPC: The lowest one corresponds to the longest drift length, the topmost to the shortest drift length. Black stars are NA49 reference data, and green, blue and red points are NA49-future data. The horizontal axis on each plot is the sector number.

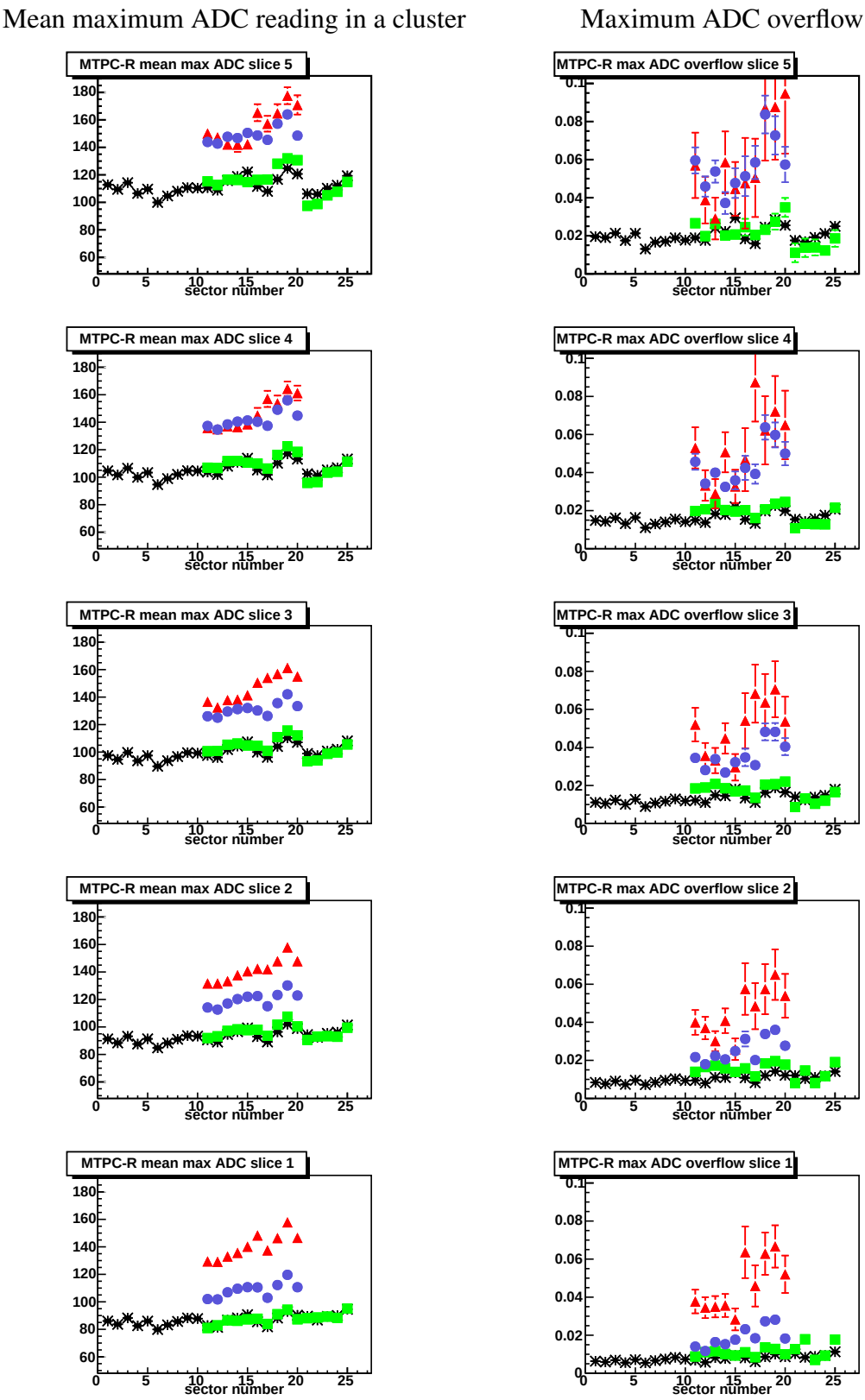

Figure 15: Maximum ADC reading in a cluster and fraction of overflowed clusters in MTPC-R. The plots represent 5 different horizontal slices of the MTPC: The lowest one corresponds to the longest drift length, the topmost to the shortest drift length. Black stars are NA49 reference data, and green, blue and red points are NA49-future data. The horizontal axis on each plot is the sector number.

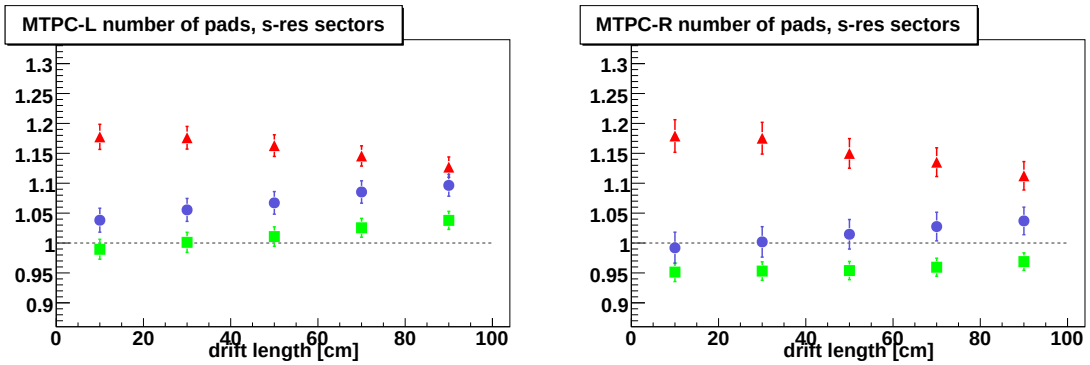

Figure 16: Ratio of number of pads in a cluster in NA49-test run and NA49 reference data in the standard resolution sectors of MTPC-L and MTPC-R as a function of drift distance. Colors correspond to three voltages on the sense wires used during NA49-future test run.

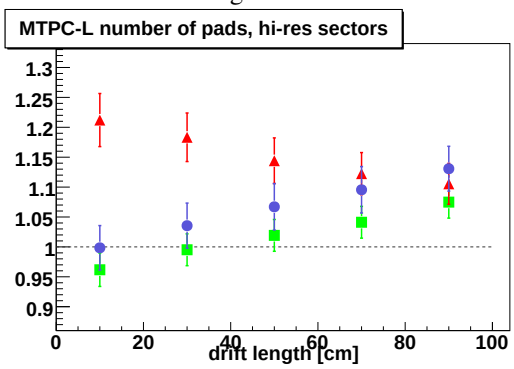

Figure 17: Ratio of number of pads in a cluster in NA49-test run and NA49 reference data in the high resolution sectors of MTPC-L as a function of drift distance. Colors correspond to three voltages on the sense wires used during NA49-future test run.

horizontal coordinate.

The values for low and middle voltage are increasing with the drift length. This means, that transversal diffusion is slightly higher in the new gas mixture. By contrast, values for the highest voltage are the highest for the shortest drift length. This suggest that the sense wires no longer work in the proportional mode: the most concentrated electrons from the shortest drift length are strongly amplified on the wires. The small amount of quencher gas allows the avalanche size to increase, increasing the dimension of the cluster.

- *Number of time slices of a cluster.* The results are presented on figs. 18 and 19. Again, normalized number of time slices for the lowest voltage (■) are the lowest and the closest to 1; however they do not drop below 0.95. Values for higher voltages (●, ▲) are above.

  The dependence on drift length is similar to number of pads case: for the low and

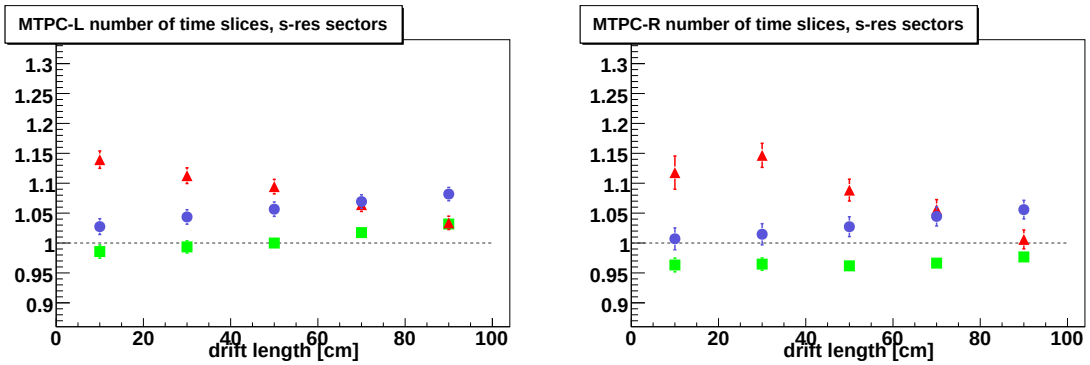

Figure 18: Ratio of number of time slices in a cluster in NA49-test run and NA49 reference data in the standard resolution sectors of MTPC-L and MTPC-R as a function of drift distance. Colors correspond to three voltages on the sense wires used during NA49-future test run.

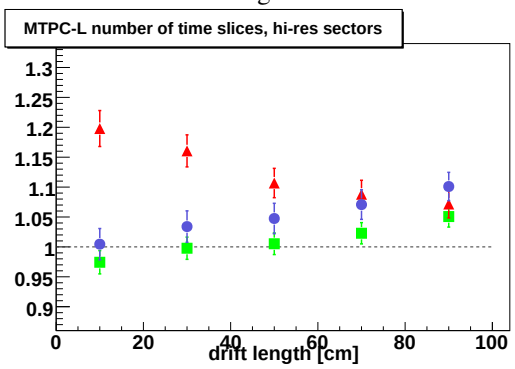

Figure 19: Ratio of number of time slices in a cluster in NA49-test run and NA49 reference data in the high resolution sectors of MTPC-L as a function of drift distance. Colors correspond to three voltages on the sense wires used during NA49-future test run.

middle voltages longitudinal diffusion increases with the drift length, while for the highest voltage lack of the quenching gas allows increase of the cluster size.

- *Maximum ADC reading in cluster.* The results are presented on figs. 20 and 21. Again, normalized ADC readings for the lowest voltage (■) are the lowest and the closest to 1, but the difference is more significant than for the number of time slices and number of pads. The values for the two higher voltages (●, ▲) are definitely above 1. This shows an increase of the gas amplification with increasing voltage on the sense wires.

  The values corresponding to the two lowest voltages decrease with the drift length. This can be explained by diffusion: the more the electrons diffuse, the less charge is concentrated in the central part of the cluster, resulting in lower maximum ADC reading. The values corresponding to the highest voltage increase with the drift length. However it is fairly well visible in the plots 13 and 15, that the values of

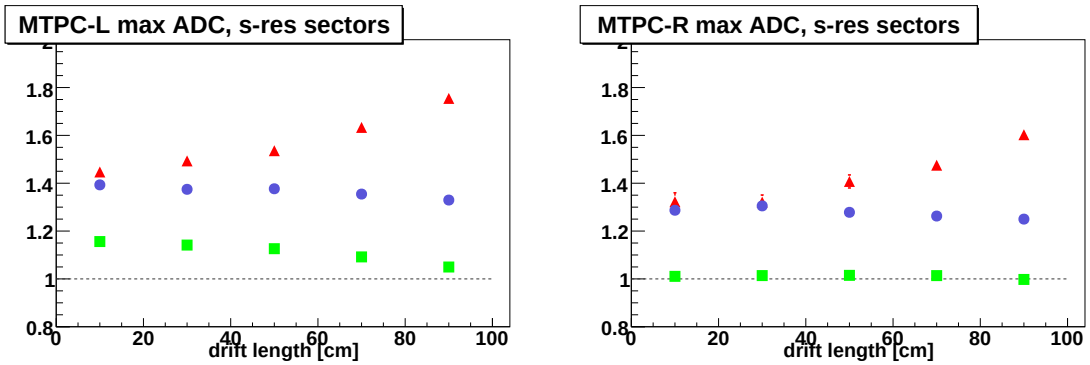

Figure 20: Ratio of maximum ADC reading in a cluster in NA49-test run and NA49 reference data in the standard resolution sectors of MTPC-L and MTPC-R as a function of drift distance. Colors correspond to three voltages on the sense wires used during NA49-future test run.

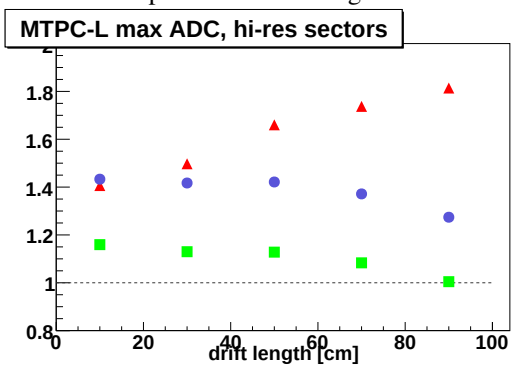

Figure 21: Ratio of maximum ADC reading in a cluster in NA49-test run and NA49 reference data in the high resolution sectors of MTPC-L as a function of drift distance. Colors correspond to three voltages on the sense wires used during NA49-future test run.

maximum ADC reading decrease with the drift length; just they decrease slower than in NA49 (∗). This is a symptom of the saturation of the gas amplification: when a big number of the positive ions is created during the gas amplification process, they shield the electric field of the sense wires, which – in turn – decreases gas amplification.

- *ADC overflow.* The results are presented on figs. 22 and 23. The difference between NA49-future and NA49 data is clearly visible. Normalized ADC overflow is the lowest for the lowest voltage (■), but sometimes it reaches even 2. On the fig. 13 one can see, that this corresponds to even 4% of overflowed clusters. Values for the higher voltages are far above.

  The values for the highest voltage (▲) increase with drift length. However – likewise in case of maximum ADC reading – this is caused by normalization to NA49 data. The plots 13 and 15 show that the overflow is decreasing with drift length, but not as

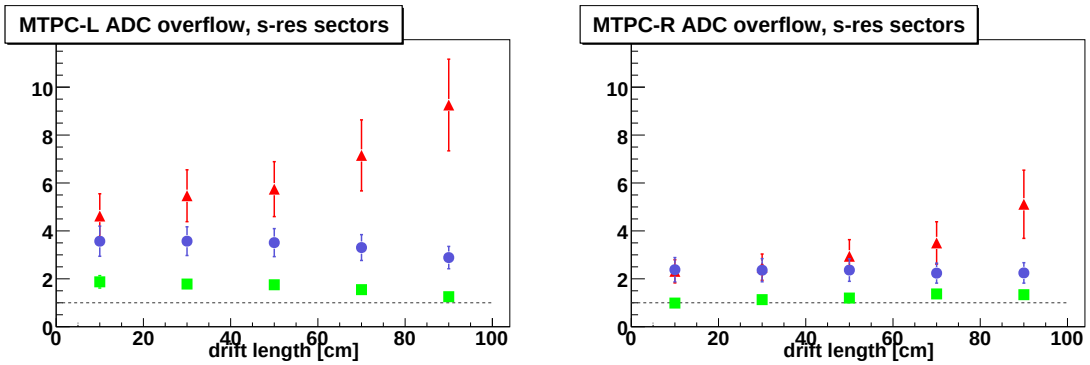

Figure 22: Ratio of fraction of overflowed clusters in NA49-test run and NA49 reference data in the standard resolution sectors of MTPC-L and MTPC-R as a function of drift distance. Colors correspond to three voltages on the sense wires used during NA49-future test run.

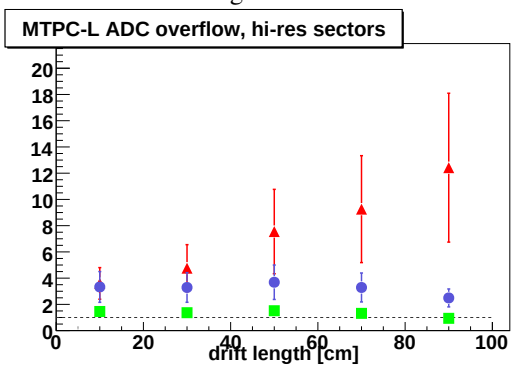

Figure 23: Ratio of fraction of overflowed clusters in NA49-test run and NA49 reference data in the high resolution sectors of MTPC-L as a function of drift distance. Colors correspond to three voltages on the sense wires used during NA49-future test run.

fast as in the NA49 data. Saturation of the gas amplification due to the positive ions shielding the sense wires can be an explanation for this observation.

2.5.3 Conclusions

For the lowest voltage values (■) the analyzed parameters ratios have the lowest and the closest to 1 values – they are the most similar to the NA49 reference data. Dependence of number of time slices and number of pads on the drift length shows, that both longitudinal and transversal diffusions are higher than in NA49. However for the lowest of the voltages used the cluster dimensions are not increased by more than 5%. This should not worsen the spatial resolution significantly. Another important observation is that the number of time slices is not lower by more than 5% in comparison to NA49 (for which it was about 6). During the NA49-future test run the signals were sampled by 512 time slices but since the first SHINE run in 2007 only 256 time slices are taken. As a result the number of time

slices in cluster decreases by half. The minimum number of time slices in cluster is 2, and 3 are enough for precise estimation of the cluster position.

The difference of maximum ADC reading for the lowest voltage is not higher than 20%. The more problematic is ADC overflow: even for the lowest voltage the overflow is up to 100% higher than in NA49. Overflowed clusters may distort results of dE/dx measurement, however separate analysis is needed in order to check whether this is a significant effect.

The values for the higher voltages (●, ▲) give worse signal quality. The cluster dimensions are higher than in NA49 which can worsen spatial resolution. Also the ADC overflow values are significantly higher: for the highest voltage they are up to 10 times higher than in NA49. This could seriously distort dE/dx measurement. These voltages are definitely too high for efficient operation of the TPCs, however it should be noted that the detector operation is still stable.

The Ar/CO_2 95/5 mixture can be used as a replacement for $Ar/CH_4/CO_2$ 90/5/5. The lowest of the voltages tested (1060V/990V) provide good signal quality and guarantee at least 40 V safety margin of stable detector operation.

3 Gas system

3.1 Principle of operation

In order to make the TPCs work properly, the gas mixture must be very pure (in particular oxygen and water content cannot be higher than tens ppm), mixture of the components must be precise and stable (order of 0.1%).

Walls of the TPCs are two layers of 125 μm thick Mylar foil in order to reduce secondary scattering. Even small (order of a few mbar) overpressure or underpressure could damage the foil. There is a bubbler connected to the TPC; it keeps a slight overpressure, prevents the air from getting into the chamber, but also protects the TPC from too high overpressure. Slight overpressure (0.50 mbar) is necessary to make the bubbler bubble constantly. The volume between two Mylar foils is flushed with nitrogen to prevent air

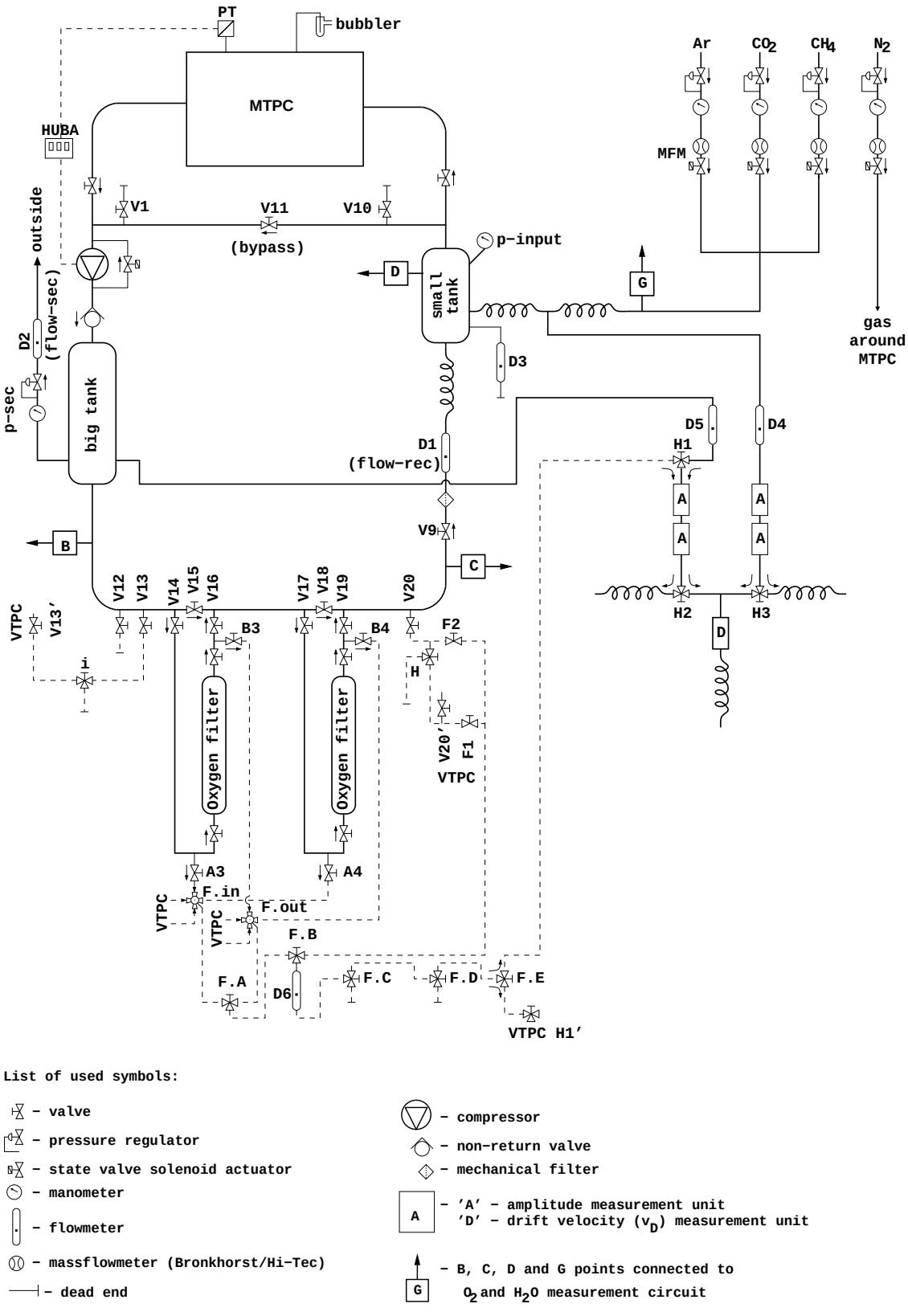

Figure 24: Schematic of the gas system circuit of one of the MTPCs. Each MTPC has an identical system, VTPCs' systems differ only by absence of CH_4 line and (not used anyhow) V10 valve. Argon input lines in VTPCs were used for neon in NA49. Pipes drawn with dashed lines are not in use currently.

diffusion into the TPC.

The structure of gas system in SHINE is shown in fig. 24. Each TPC has its own system, they are mounted in two racks: one for MTPC-L and VTPC-1, the second for MTPC-R and VTPC-2. This allows pairs of systems to share oxygen and water content meters.

The mixture of the gas coming into the system is set using separate massflowmeter for each component. The compressor makes the gas circulate through the gas system. The gas leaving the chamber is recirculated through the oxygen filter and injected back to the TPC. 85-90% of the gas is recirculated – only small fraction of fresh gas is needed to maintain clean gas mixture. The overpressure in the TPC is monitored using the *HUBA* instrument. Compressor frequency is automatically regulated by the *Danfoss* frequency converter in order to maintain constant overpressure.

Quality of the gas is monitored using oxygen and water content meters (described in appendix section A.5), also gas amplification and drift velocity is measured (described in section A.6).

GAP TPC has much more simpler system. The fresh gas mixture is flushed through the chamber. There is no recirculation and filtering system, nor the measurement units. The walls are one layer of Mylar foil.

3.2 Modes of operation

Gas system can be operated in 4 modes: hibernation, recirculation, purge and *bypass* recirculation.

3.2.1 Hibernation

This mode is applied when the detector is not used for a longer time. To prevent the air from leaking into the chamber, pure nitrogen is supplied – nitrogen is much cheaper than the gases used during normal operation. The gas is put into the chamber with flux of 200 l/h for MTPC and 50 l/h for VTPC and it comes out through the bubbler. The compressor and recirculation circuit are not used.

3.2.2 *Bypass* recirculation

Initialization of the compressor may cause sudden pressure instability that could be dangerous for the walls of the chamber. Therefore the input and output valves of the chamber are closed, and the valve V11 bypassing the chamber is open; also the recirculation valve V9 is open. The chosen gas mixture is set and the fresh gas flow is increased to normal value: about 500 l/h (MTPC) and 120 l/h (VTPC). When pressure in the small tank reaches 500 mbar the compressor is being turned on.

Pressure in the circuit is regulated by the valve *p-sec* controlling the gas outflow from the circuit, and by the recirculation valve V9. When the pressures are stable, TPC is open and the bypass circuit is closed.

3.2.3 Purge

If the gas mixture is contaminated or it needs to be changed (especially after hibernation with nitrogen) it is necessary to apply the purge procedure. The fresh gas flux is set to about 3400 l/h (MTPC) or 900 l/h (VTPC). Gas from the chamber is pumped out via *p-sec* valve. Usage of recirculation circuit is minimal. Valve V9 is just slightly open, to clean the gas in the recirculation circuit also. The oxygen filters are not used.

3.2.4 Recirculation

When the chamber is filled with the selected gas mixture, the standard recirculation mode can be started. In this mode flow of the gas through the chamber is the same as in the purge mode, but most of the gas getting out from the TPC is recirculated through the oxygen filters and put back to the chamber. Only 10-15% of the fresh gas is put to the circuit.

3.3 Operation of the system during the run in 2007

3.3.1 Oxygen and water content measurement

Oxygen and water content can be measured using the system described in appendix section A.5. The oxygen and water content during the run in 2007 is shown in fig. 25. The oxygen

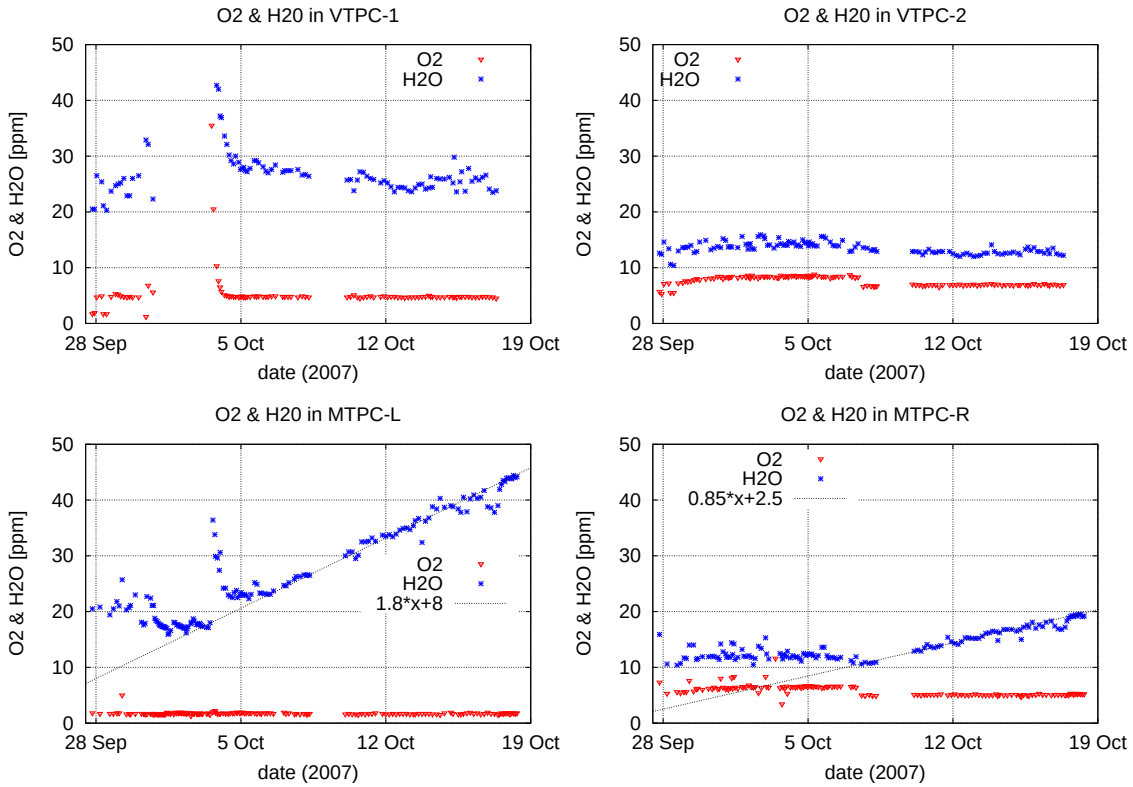

Figure 25: The readings from oxygen and water meters in the four TPCs during the run in 2007. The reading was done in point *B* (gas coming out from the TPC) in each of four systems. Lack of points between 30 September and 3 October in VTPC-1 is caused by few days pause in recirculation. Sudden increase of water content is also visible on the MTPC-L plot, because these two chambers use the same meters.

content in VTPC-1 and MTPC-L is lower than in VTPC-2 and MTPC-R, while water content is higher. This means, that the differences are caused by the systematic shift in the meters rather than by the real contamination differences (these pairs of the chambers use the same meters).

From about 7 October the water content in both MTPCs began to rise linearly with time. This shows that the filters can effectively remove only limited amount of water from the gas. The flow of the gas in the MTPCs' circuits is about 4.5 times higher than in the VTPCs'. Assuming that the contamination is proportional to the flow, this explains why the effect has not became exposed in VTPCs during one month period. Water content below 100 ppm is still acceptable and does not affect signal quality significantly.

Between 8 and 10 October the flow in the VTPC-1 system was reduced and the gas was not recirculated through the filters due to failure of *Danfoss* frequency converter supplying power to the compressor. The oxygen and water content could not be measured during

that time. When the system was turned back to operation, the measured oxygen and water content was very high, which is clearly visible on the plot. VTPC-1 had to be purged in order to purify the gas. The sudden increase of water content visible on the plot for the MTPC-L is caused by the fact that the both TPCs use the same meter units. The readings were taken too often and during measurement of water content in the MTPC-L the gas in the meter was still contaminated with water from the VTPC-1 circuit.

3.3.2 Drift velocity measurement

The drift velocity can be monitored using the counters described in appendix section A.6. The measurements from the beginning of the run in 2007 are shown in fig. 27. The temperature, drift voltage in the meters and the reciprocal of air pressure is shown in fig. 26.

The big changes (especially in the MTPCs) of the drift velocity at the beginning of the run are caused by the fine tuning of the gas mixture in order to achieve proper drift velocity. Also the drift voltage in the meters was changed on 18 October in order to make the measured drift velocity closer to the drift velocity in the TPC for easier monitoring.

The red stars on the plots represent the drift velocity measured directly in the meters. It is strongly correlated with the reciprocal of air pressure, which is proportional to the gas density. The blue circles represent so called "corrected" drift velocity. The correction is done for the air pressure, temperature and drift voltage in the meters. The corrected drift velocity seems to be independent of the air pressure demonstrating proper work of the correction algorithms. Also the constant parts of the corrected drift velocity demonstrate the accuracy of the measurement – about 0.01 cm/μs.

However, the proper methodology of the measurement is not fully understood yet. Analysis of residuals in MTPCs shown that the reconstructed clusters are systematically shifted from the fitted tracks, and the shift is linearly increasing with the drift length. This means, that the measured values of drift velocity are wrong. In order to obtain proper values of drift velocity, they are multiplied by correction factors calculated using the residuals analysis.

The values of correction factors calculated are shown in fig. 28. The error of the mea-

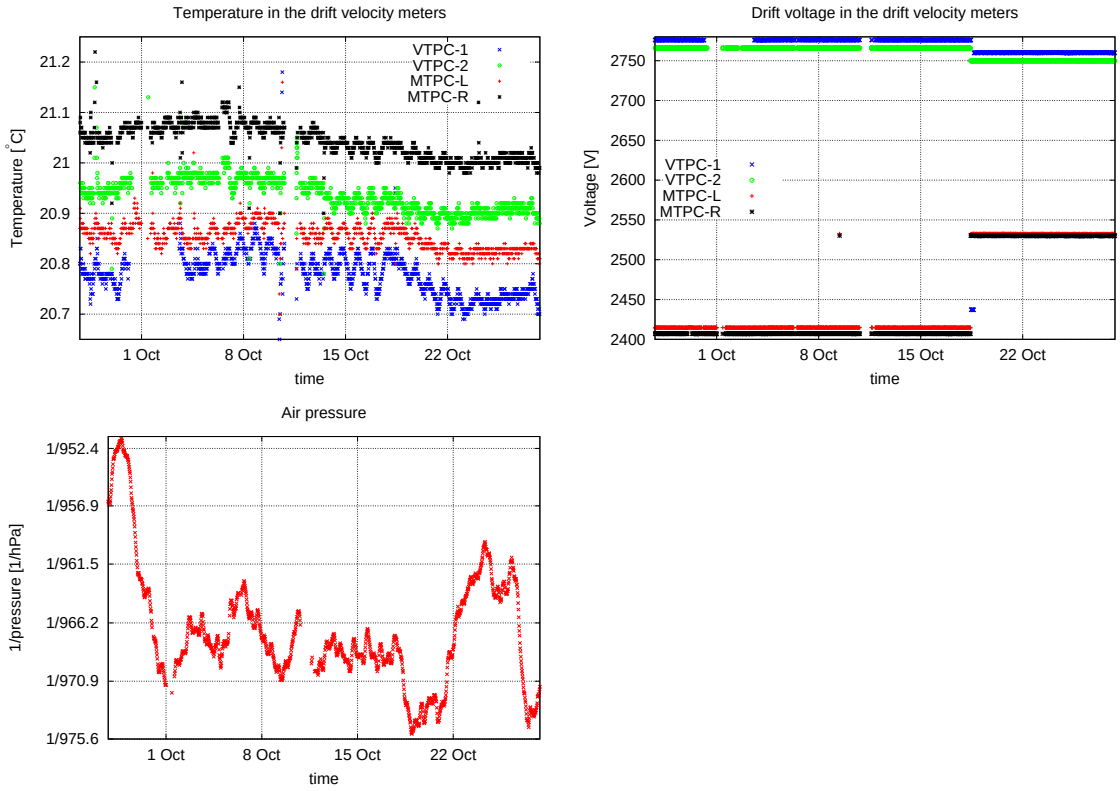

Figure 26: Air pressure, temperature and drift voltage in the drift velocity meters during the SHINE run in 2007.

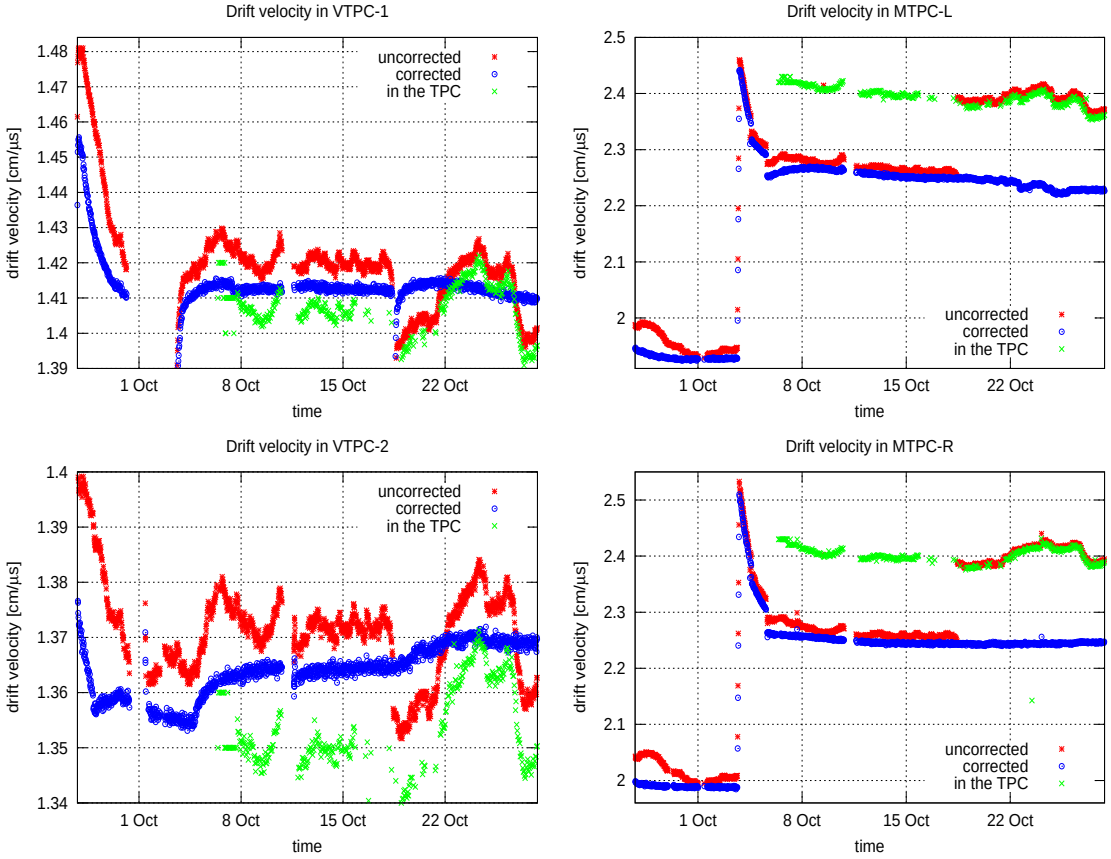

Figure 27: Uncorrected and corrected drift velocity measured during the SHINE run in 2007. The big variations at the beginning are caused by fine tuning of the gas mixture. The variations after 8 October are described in detail in the text.

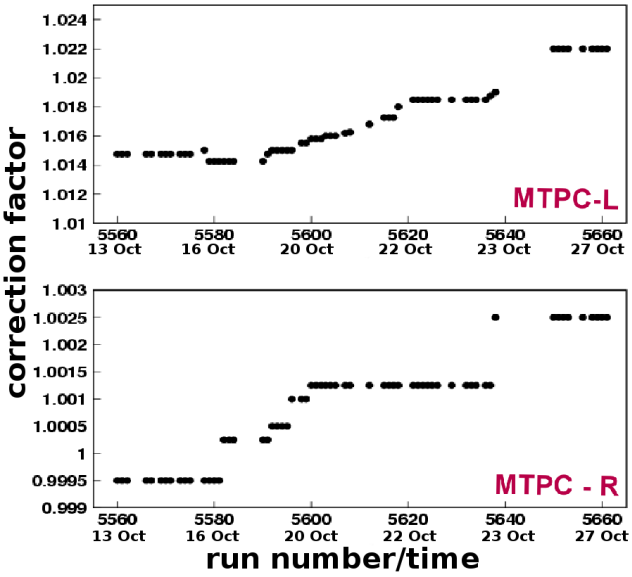

Figure 28: Correction factor applied to the measured drift velocity in MTPCs as a function of run number. The drift velocity measured in the measurement units was lower than in reality. This effect has to be understood and eliminated. The "run number" on the abscissa is not linear function of time, but it represents period of SHINE run in 2007.

surement increases with time. The error of the measurement extends up to 2% in MTPC-L. This corresponds to 2 cm error of position measurement for the longest drift lengths. The error is very high – the typical uncertainty of a cluster position in NA49 was a fraction of millimetre.

The correction factor shown on the plot is higher than one in most of the runs – the measured drift velocity is lower than real drift velocity in TPC. Also, the values of the corrected drift velocity in the MTPCs shown on fig. 27 decrease with time. There are a few possible explanation of this problem:

- The gas mixture was changing during the run. It is unlikely that the massflowmeters operation was unstable. However, if after the purge the setting of the fresh gas mixture was slightly different from the mixture in the TPC, the mixture in the TPC would change slowly. In such case the "E/p/T" curve (see section A.6 and fig. 31) used for calculating the drift velocity in the TPC would lead to wrong values. The curve has been measured in 11 October last time. Probably it should be measured more often.

- The temperatures shown in fig. 26 start to decrease after 17 October. This is correlated with increase of error of drift velocity measurement. It is possible that the

algorithms used for calculation of the drift velocity in the TPCs does not apply correction for the temperature properly.

- The flow of gas through the meters was too small. The gas for the measurement is sampled from the recirculation circuit and exhausted to the air after passing through the drift velocity detector (as it is shown in fig. 24). If the gas flow was too low, air could diffuse into the detector through the output pipe. Contamination of air – composed mostly of nitrogen – in the gas in the detector could decrease measured drift velocity. It is however unclear why the effect was increasing during the time of run. It could be caused by ill-conceived manipulation of the gas flow through the meter.

- The pressure in the meters was higher than the atmospheric pressure. During the run in 2007 new filters were put at the output pipes of the meters. The filters were required to fulfill the radioactive safety conditions, but they were never used before in the experiment. If the filters blocked the gas from getting out of the meters, the pressure in the meters would increase, resulting in higher gas density and thus lower drift velocity.

These possibilities will be investigated before the next run.

4 Discussion and conclusions

The main conclusion of this paper is the positive result of the analysis of the signal properties with the new gas mixture in the MTPCs. Satisfactory results obtained during the test run convinced the collaboration to use the mixture in the experiment. The absence of methane solves the security and technical problems related to using flammable gas mixture.

The analysis of the data from the test run showed that the parameters of the signal for the new gas mixture are comparable to the ones for the standard gases of NA49. Only the ADC response differs significantly, but it can be corrected by adjusting (lowering) the value of the high voltage on the sense wires. The measurements done with the higher voltages on the sense wires show that the MTPCs operate correctly with the high voltage margin of at

least 40 V below the discharges. During the first run of SHINE no problems were observed that could be caused by the new mixture.

TPCs used in SHINE are 13 years old. They were operated for 7 years by NA49, then they were unused for 4 years. After completion of NA49 data taking they were inspected and some minor repairs were done (just a few wires were broken). TPCs worked properly during the NA49-future test run and the first run of SHINE. The upgrade of TPC readout and data acquisition is in progress. The detector should be functional until SHINE data taking is finished.

The gas system is in good condition. It has been made of high quality parts (steel pipes, vacuum valves) that seem to resist ageing effects. The only serious problem that occurred during the run in 2007 was fault of one of *Danfoss* frequency converters. It caused 3 days break in operation of VTPC-1, but finally the device was replaced without problems.

The drift velocity measurement needs to be understood better before the next run. Although to a certain degree the drift velocity can be obtained from the analysis of the data from the TPCs, the proper measurement in the gas system is important in order to achieve reliable results.

Currently an analysis of space uncertainties of cluster is being done. NA49 uses complex formulae to describe the uncertainties: there is separate parametrization for each TPC (independent for high resolution, standard resolution and standard resolution prime in MTPCs) and it is a function of number of pads in a cluster, drift length and angle between track and pad plane and pad tilt angle. Since the gas mixture is changed in SHINE, parameters of diffusion and pad response may be different than in NA49. Goal of the analysis is to extract the new uncertainties from the new data.

5 Acknowledgements

I would like to thank Wojciech Dominik for supervision of this thesis. I thank Rainer Renfordt for substantial and linguistic help. I would also like to thank whole NA61 and NA49 collaborations for a possibility of participating in the experiment and for the indispensable experience I have gained.

A Appendix: Parts of the gas system

A.1 Gas supply

Nitrogen is standard gas supplied by CERN – it is easily accessible, and many experiments use it. It is stored in liquid form in the large Dewar near the experimental hall. Argon is supplied on demand. If sufficiently large amounts of the gas are ordered it is also stored in liquid form – it is much cheaper than in gaseous form. In case of SHINE cooperation with the COMPASS experiment allowed to order liquid argon. CO_2, neon and methane are available in gaseous form only. They are stored in smaller volume bottles near the experimental hall.

A.2 Massflowmeters

Flow of each of the gases coming into the circuit is controlled by the massflowmeters (drawn in the top right part of fig. 24). They are used for setting the mixture of Ar, CO_2 and CH_4 inside the TPC, the fourth massflowmeter controls flow of nitrogen to the protection volume around the TPC.

Due to calibration uncertainty, flow of each gas can be set only with accuracy of 1% of maximum flow. However, once the flow is set, it is stable with much better accuracy. The argon/neon and CO_2 massflowmeters of VTPCs and MTPCs have been calibrated before the first SHINE run in 2007.

A.3 Compressor and recirculation system

In order to achieve desired purity of gas inside TPC, flow of about 3500 l/h (MTPC) and 800 l/h (VTPC) is needed. Such big amounts of gas cannot be simply flushed out through the bubblers. The gas is pumped out from the TPCs by the compressors. Each compressor is controlled by *Danfoss* frequency converter. Pressure in the TPC is measured by *HUBA Control* device – frequency of the compressor is adjusted automatically in order to achieve 0.50 mbar overpressure in the TPC with accuracy and stability of 0.01 mbar.

A.4 Oxygen filters

The filters are about 1.5 m long and 10 cm in diameter tubes with active copper insert. While the gas is flowing through the filter, copper oxidizes removing oxygen from the gas. The filter can take about 6.3 liters of gaseous oxygen which corresponds to a few months of usage in typical conditions. Also during the first weeks of usage, the filter reduces the water content in the gas. When the filter becomes saturated and its cleaning efficiency decreases, it is regenerated in the separate system described in section B.

While each of the four TPCs needs only one filter, there are six filters in the system – two are spare, they can be regenerated while the system is operating. Also each system has two slots for the filters. The filter replacement can be done smoothly, with a minimal disturbance of the system operation.

A.5 O_2 and H_2O monitor units

There are four points in each system (named *B*, *C*, *G*, *D* in fig. 24) where oxygen and water content in gas can be measured. Circuit of the connection is presented on fig. 29. There are only 2 sets of measurement units for 4 TPCs: there is one set in the VTPC-1/MTPC-L rack and one in the VTPC-2/MTPC-R rack. Hence the gas from only two TPCs can be measured at the same time. Also the gas needs some time to get from the main circuit to the measurement units. For this reason the measurement points cannot be switched more often than once per half an hour or even longer if the contamination in the two TPCs differ a lot. The measurement points are switched manually, also the readout is not automatic: it has to be done by the shift crew.

The measured gas can be taken from one of the four points of each system:

G: fresh gas mixture, which is clean and can be used as a reference,

B: gas coming out from the TPC, to estimate contamination inside the chamber,

C: gas that has passed through the filter, to control filtering effectiveness,

D: gas entering the TPC.

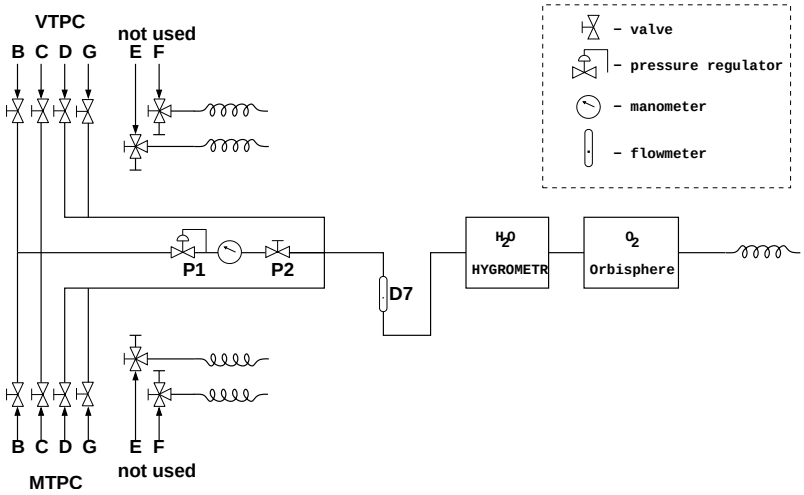

Figure 29: Schematic of a circuit leading gas to the oxygen and water meters. There are only two pairs of the meters in the whole system. They are shared between MTPC-L/VTPC-1 and MTPC-R/VTPC-2. Gas can be taken from 4 points (B, C, G, D) of each system, but only one at the time.

A.6 Gas amplification and drift velocity measurement

The measurement units are marked with "A" and "D" letters on the right side of fig. 24. Gas amplification and drift velocity can be measured in two points of the system: fresh gas and gas coming out from the TPC. There are 4 gas amplification measurement units in each system so the gas from both points can be measured simultaneously. The measurement is very precise, and basically stable, but sometimes the measured values jump spontaneously. Two units in each point allow for more reliable measurement. There is 1 drift velocity unit in each system so it has to be chosen at which point to measure.

The units are located in air-conditioned part of racks to guarantee stable temperature. Readout is done using electronic system located in control room. The results are displayed immediately on a computer screen allowing the shift crew to monitor the gas quality easily. The computer is part of a bigger system called *slow control*; values of the drift velocity are sent to the data storage together with physics data from other parts of the detector.

- **Gas amplification** measurement units are single wire detectors with ^{55}Fe source. ^{55}Fe decays by electron capture producing 5.9 keV and 6.5 keV x-rays. The photons ionize the gas causing gas amplification avalanche near the wire. Electromagnetic impulse is induced on the cathode, then it is amplified electronically and its amplitude is measured.

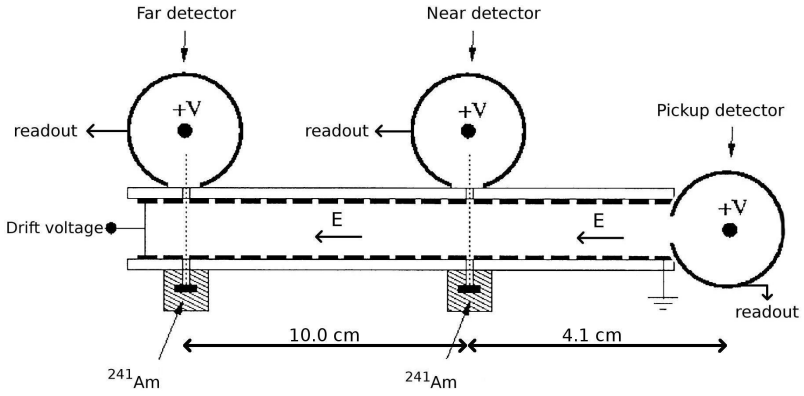

Figure 30: Schematic of drift velocity measurement unit.

The "slow control" computer normalizes the measured values for the temperature changes, hence the measurement is sensitive only to the gas mixture changes. The measurement is very sensitive to even small changes of gas mixture, thus it allows for very precise monitoring of gas mixture stability. Relative stability of the measurement is lower than 1%. Even slightest modification of gas mixture can be recognized.

- Schematic of the **drift velocity** measurement unit is presented in fig. 30. The unit consists of 3 single wire counters called "far", "near" and "pickup", two ^{241}Am sources located near the "far" and "near" counters, and drift cage with homogeneous electric field. When one of the sources emits an α particle, it is being registered in the "far" or the "near" counter. Also, the particle ionizes gas in the drift cage. Electrons from the ionization drift in the electric field and are registered in the "pickup" counter. This way one can calculate time t_n that electrons takes to drift from the "near" to the "pickup" counters, or t_f from the "far" to the "pickup" counters. The distance between "far" and "pickup" counter d_f = 14.1 cm; the distance between "near" and "pickup" counters d_n = 4.1 cm. Using these values drift velocity can be calculated with the following formula:

$$v_d = \frac{d_f - d_n}{\langle t_f \rangle - \langle t_n \rangle}. \tag{3}$$

Measured values are used to estimate the drift velocity in the TPC. To do it, first the drift velocity is measured in wide range of drift voltages. The results are plotted on

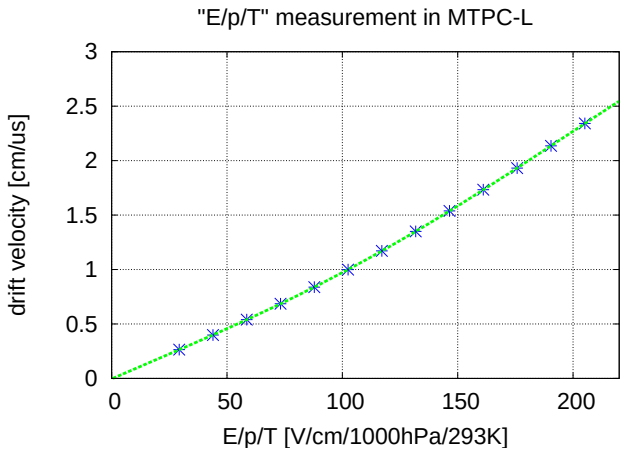

Figure 31: Example of the measurement of drift velocity versus $E/p/T$ in the MTPC-L gas. The drift velocity is measured for various reduced drift field values. The pressure is normalized to 1000 hPa, the temperature in the meter to 293 K. A curve fitted to the measured points is used to calculate drift velocity in the electric field in the TPC.

v_d versus $E/p/T$ graph, where E is electric field and p is air pressure. A polynomial is fitted to the values. An example of result of such measurement is presented in fig. 31. This polynomial is used later to extrapolate measured drift velocity to the chamber, corrected for temperature, pressure and drift voltage changes both in the TPC and the measurement unit.

B Appendix: Oxygen filter regeneration

The filters are regenerated in a special unit. Regeneration is done by flushing Ar/H_2 (98/2) mixture through the filters in temperature 200°C for a few days. Hydrogen from the mixture attaches to the oxygen in the filter creating water particles that leave the filter with the gas. *MCM* moisturemeter unit located at the output of the filter allows monitoring the regeneration process.

The first filter regeneration in SHINE has been performed before the run in 2007. The readings from moisturemeters are presented in fig. 32. Since the gas used for regeneration does not contain water, water content on the output of the filter equals amount of removed oxygen plus the water trapped in the filter. All 6 filters have been regenerated, although two of them (1 and 3) have been already regenerated in 2003 and not used from that time. It turned out that they are in perfect condition – even better than the other filters at the end of

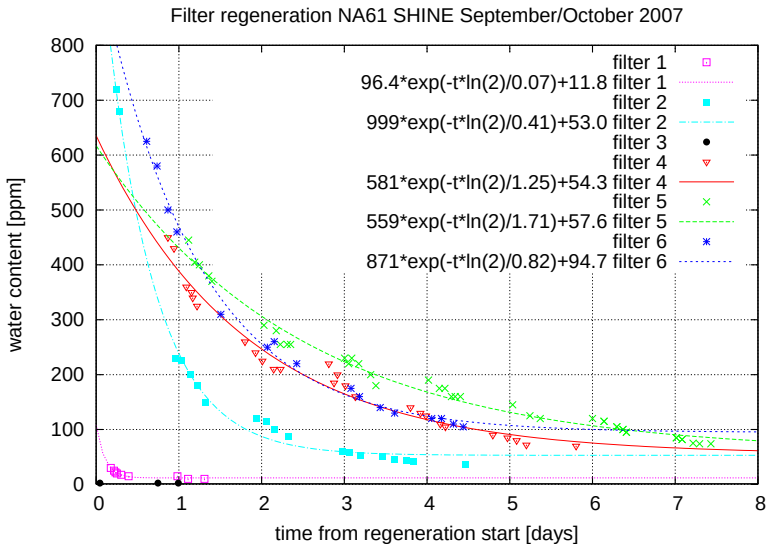

Figure 32: Water content in gas coming out from a filter during regeneration as a function of regeneration time. An exponential function describes the data quite well, however one can see, that the water content goes down faster during daytime (the data on the plot have been taken mostly between 9 a.m. and 7 p.m., missing parts are nights). This was caused probably by higher air humidity during nights. Filters 1 and 3 (points in the bottom left corner) have been already regenerated in 2003.

regeneration. This is probably because gas with a higher hydrogen content (most probably 7%) was used in NA49 for regeneration. Using lower hydrogen content may require longer regeneration time. On the other hand using gas with high hydrogen content is dangerous. Using 2% mixture allows to avoid security issues.

The estimated amounts of oxygen removed from each filter are shown in table 5. One can see significant differences between the filters. They seem to be independent of number of times each filter was regenerated in the past. Also, the measurement is not very precise. Capacity of a filter written in logbook in 1995 equals 6.3 l of gaseous oxygen. This contradicts high values shown in the table. However part of the water content at the filter output comes from the water trapped in the filter. This could cause overestimation of the removed oxygen values.

Cleaning the filter to 100 ppm of water on the filter output takes 2-7 days. Filters 1, 3, 4 and 5 have been used during SHINE run in 2007. Fig. 25 demonstrates that they removed oxygen properly for over 30 days of the run.

Table 5: Summary of regeneration of oxygen filters before the first SHINE run in 2007. Amounts of (gaseous) oxygen removed from each filter are obtained by integrating measured water content in the gas at the output of each filter. Filters 1 and 3 have been regenerated in 2003 and not used from that time – this is why amounts of removed oxygen are very small.

Filter number	total number of regenerations	regeneration time [days]	oxygen removed [l]
1	6	1.3	0.12
2	6	4.5	4.0
3	5	1.0	0.01
4	4	5.8	6.3
5	4	7.4	8.3
6	4	4.4	6.8

References

[1] NA61/SHINE web page: http://na61.web.cern.ch.

[2] M. Gaździcki for the NA49 Collaboration. Report from NA49. *Journal of Physics G*, 30:S701, 2004, [arXiv:nucl-ex/0403023v1].

[3] W.-M. Yao et al. Review of Particle Physics. *Journal of Physics G*, 33, 2006.

[4] S. Afanasiev et al. The NA49 large acceptance hadron detector. *Nuclear Instruments and Methods in Physics Research A*, 430:210–244, July 1999.

[5] T. Alber et al. Transverse Energy Production in ^{208}Pb + Pb Collisions at 158 GeV per Nucleon. *Physical Review Letters*, 75(21):3814–3817, November 1995.

[6] N. Antoniou et al. Study of hadron production in collisions of protons and nuclei at the CERN SPS, NA49-future letter of intent. *CERN-SPSC-2006-001*, 2006. SPSC-P-329.

[7] M. Gaździcki. A new SPS programme. *Proceedings of Science*, PoS(CPOD2006)016, 2006.

[8] M. Kowalski. Rozprawa habilitacyjna (habilitation thesis) "Komory Projekcji Czasowej w Eksperymentach na Wiązkach Relatywistycznych Jonów". Instytut Fizyki Jądrowej im. Henryka Niewodniczańskiego w Krakowie, October 2001.

[9] F. Sauli. Principles of Operation of Multiwire Proportional and Drift Chambers. *CERN-77-09*, page 41, 1977.

[10] A. Peisert and F. Sauli. Drift and Diffusion of Electrons in Gases: a Compilation. *CERN Report 84-08*, page 29, July 1984.